Polymer Degradation and Stability 222 (2024) 110708

Contents lists available at ScienceDirect

Polymer Degradation and Stability

journal homepage: www.journals.elsevier.com/polymer-degradation-and-stability

Degradation processes in polyolefins with phenolic stabilizers subjected to ionizing or non-ionizing radiation

Miroslav Šlouf [a], Veronika Gajdošová [a], Ivana Šloufová [b], Miroslava Lukešová [a], Danuše Michálková [a], Michael Thomas Müller [c], Jan Pilař [a,*]

[a] Czech Academy of Sciences, Institute of Macromolecular Chemistry, Heyrovského nám. 2, 16206 Praha 6, Czech Republic
[b] Faculty of Science, Department of Physical and Macromolecular Chemistry, Charles University, Hlavova 2030, 128 40 Prague 2, Czech Republic
[c] Leibniz-Institut für Polymerforschung Dresden e.V. (IPF), Hohe Str. 6, Dresden 01069, Germany

ARTICLE INFO

Keywords:
High-density polyethylene (HDPE)
Cycloolefin copolymer (COC)
Natural phenolic stabilizers
Spin adducts of polymer radicals to TTBNB
Polymer photodegradation
Accelerated weathering
e-beam irradiation
Electron spin resonance imaging
IR microspectroscopy
ATR FTIR spectroscopy

ABSTRACT

We investigated degradation processes in polymer plaques made of polyolefin (HDPE or UHMWPE or COC) prepared by melt-mixing with or without phenolic stabilizer (natural α-tocopherol or synthetic Irganox®1010) and spin trapping agent (TTBNB; 2,4,6-Tri-tert-butylnitrosobenzene). The degradation was initiated either by *low-energy, non-ionizing radiation* (wavelengths corresponding to terrestrial range of solar UV radiation) or *high-energy, ionizing radiation* (electrons accelerated at 1.5 MeV). The motivation for the study was our recent finding that some phenolic stabilizers exhibited a surprising *pro-oxidant activity* in polyolefins subjected to non-ionizing radiation. Consequently, we asked if the phenolic stabilizers in polyolefins behave in the same way during long-term, low-energy, non-ionizing UV irradiation and after short-term, high-energy, ionizing e-beam irradiation. All samples were characterized thoroughly by means of electron spin resonance (ESR; the information about radiation-induced radicals), infrared microspectroscopy (IR; the detection of oxidation products and structural changes), instrumented microindentation (MHI; local mechanical properties) and light and electron microscopy (LM and SEM; surface morphology). The results proved that (i) the degradation processes in polyolefins subjected to non-ionizing or ionizing radiation were different, (ii) the phenolic stabilizers exhibited mostly their expected antioxidant activity, while pro-oxidant activity was detected only for specific conditions and/or systems subjected to non-ionizing radiation, and (iii) the selected spin trapping agent, TTBNB, was stable enough to survive standard sample preparation by melt-mixing and catch short-living unstable radicals.

1. Introduction

Our recent research has been focused on the activity of natural stabilizers during the photooxidation of polyolefins [1–3]. The investigation comprised three phenolic stabilizers: α-Tocopherol (α-Toc), the most biologically active component of vitamin E, phenolic antioxidant (+)-catechin (CAT), and synthetic stabilizer Irganox®1010 (Irg1010). All experiments were performed with three polyolefins: high-density polyethylene (HDPE), ultrahigh molecular weight polyethylene (UHMWPE), and cycloolefin copolymer (COC; a copolymer of ethylene and norbornene). These polymers were selected for two reasons: (i) they cover quite broad range of properties HDPE and UHMWPE are a ductile semicrystalline polymer *above* its glass transition temperature (T_g), while COC is a stiff amorphous polymer *below* its T_g and (ii) their structure and IR spectra are simple enough (namely in the case of HDPE and UHMWPE) to monitor structure changes in a sufficient detail.

The three recent studies [1–3] showed several interesting and/or surprising facts: Firstly, it has been demonstrated that phenolic stabilizers in polyolefins subjected to photooxidation (WOM) can exhibit pro-oxidation activity. This was in clear contrast with parallel control experiments with polymers stabilized with hindered amine stabilizer (HAS) Tinuvin®770 (Tin770). Secondly, the results have indicated that the stability of the radicals generated during photooxidation is closely connected with the mobility of the polymer chains, which is linked with glass transition temperature. Thirdly, we have successfully employed the spin trapping agent 2,4,6-tri-tert-butylnitrosobenzene (TTBNB), which was stable enough to survive sample preparation by melt mixing and to catch some very unstable, short-living polymer radicals in polymer systems with CAT stabilizer.

The surprising pro-oxidant activity of phenolic stabilizers in polymer

* Corresponding author.
E-mail address: pilar@imc.cas.cz (J. Pilař).

https://doi.org/10.1016/j.polymdegradstab.2024.110708
Received 9 November 2023; Received in revised form 24 January 2024; Accepted 16 February 2024
Available online 17 February 2024

systems have been confirmed by a few other researchers recently. All studies seem to agree that the pro-oxidant behavior of phenolic stabilizers (which are either natural or synthetic antioxidants) occurs only under a very specific combination of circumstances, such as our case of non-polar environment (polyolefins) combined with specific degradation type (photooxidation induced by non-ionizing radiation). Recent review of Dintcheva et al. [4] concluded that numerous natural antioxidant molecules (nAO, such as phenols, polyphenols, vitamins, and carotenoids) protect most polymers against both thermooxidation and photooxidation, but when nAO's are combined with some biopolymers at higher concentration, they can act as pro-oxidants. Mukai et al. [5] measured aroxyl radical scavenging rate constants of natural antioxidants (α-Toc and three catechins: epicatechin, epigallocatechin, and epigallocatechin gallate) in ethanol solution; the result indicated that the α-Toc exhibited a pro-oxidant activity, which was suppressed at presence of catechins. [6] have observed that five different natural phenolic compounds derived from flavonoids (chrysin, quercetin, hesperidin, naringin, and silibinin) exhibited various levels of antioxidant activity in polypropylene, depending on the degradation type (thermooxidation vs. photooxidation) and composition (flavonoid type and concentration); signs of a weak pro-oxidant activity were detected during photooxidation. It is also worth mentioning that several research groups [7–9] employed the same spin-trapping agent like us (TTBNB; 2, 4,6-tri-tert- butylnitrosobenzene) in detecting short-living primary or secondary radicals generated during various degradation processes in solid polymer systems.

In this paper, we further extended the above-listed studies about the varying activity of phenolic antioxidants in polyolefins during polymer degradation. Foremost, we decided to compare the degradation of polyolefins subjected to non-ionizing radiation (terrestrial range of UV radiation; like in our previous papers) and ionizing radiation (high-energy electron beam). Moreover, we combined TTBNB spin trapping agent with the other two phenolic stabilizers, α-Toc and Irg1010. Additionally, we tested not only HDPE and COC (i.e. the low-T_g and high-T_g polyolefin), but also UHMWPE (ultrahigh molecular weight polyethylene). UHMWPE is available in the form of pure, medical grade, additive-free powder Chirulene 1020 [10]. The HDPE and UHMWPE polymers differ mostly by their molecular weight, but α-Toc may exhibit *prooxidant* activity in HDPE subjected to non-ionizing radiation or *antioxidant* activity in UHMWPE subjected to ionizing radiation, as discussed below.

The high-frequency ionizing radiation (such as γ-rays or e-beams with energies in keV or MeV range) carries sufficient energy to remove electrons from atoms and molecules of materials and, as a result, to create polymer alkyl radicals $P^{\bullet}$ detectable by ESR directly [11–13]. The low-frequency non-ionizing UV radiation (energies below 10 eV), simulating the terrestrial range of solar radiation, does not have enough energy to remove electrons from atoms or molecules, but it can create alkyl radicals indirectly [14]. It is supposed that during WOM aging the applied UV radiation activates so-called *chromophoric centers* in the polymer (such as unsaturated bonds, oxygenated structures, catalyst residues) [14–16], which give rise to polymer alkyl radicals $P^{\bullet}$. The polymer alkyl radicals generated by non-ionizing radiation may differ from the radicals generated by ionizing radiation and can be hard to detect by ESR [14–16]. Generation of the radicals that trigger chain photooxidation reaction in the presence of oxygen [17–22] was proved by the detection of nitroxides created during an antioxidant activity of HAS [23–26].

The principal question we address in this contribution is, if the phenolic stabilizers in polyolefins behave in the same way during (long-term, low-energy, non-ionizing) UV irradiation and after (short-term, high-energy, ionizing) e-beam irradiation. While our previous results [1–3] have demonstrated that phenolic stabilizers can exhibit *pro-oxidant activity in polyolefins subjected to non-ionizing radiation*, numerous studies have documented [27,28] that α-Toc shows *antioxidant activity in UHMWPE modified with ionizing radiation*. Moreover, we wanted to verify if the TTBNB spin trapping agent applied in combination with the other two phenolic stabilizers, α-Toc and Irg1010 can catch the unstable radiation-induced radicals, which could not be detected in the previous studies. To the best of our knowledge, this is the first systematic comparison of antioxidant and pro-oxidant activity of phenolic stabilizers in polyolefins considering the radiation type (UV radiation vs. e-beam).

2. Experimental

2.1. Materials

2.1.1. Polymers

Additive-free high-density polyethylene (HDPE), ultrahigh molecular weight polyethylene (UHMWPE) and cycloolefin copolymer (poly (ethylene-co-norbornene) (COC) were employed in this study. HDPE was obtained from Unipetrol RPA Litvinov, Czech Republic, as a non-stabilized powder of semicrystalline homopolymer 3909H ($M \sim 1 \times 10^5$ g/mol, density 0.935 g/cm^3, $T_g \sim -125$ °C). UHMWPE was obtained from Celanese, Germany as a non-stabilized powder of GUR 1020 ($M \sim 4 \times 10^6$ g/mol, density 0.934 g/cm^3, $T_g \sim -110$ °C). COC was bought from Advanced Polymers GmbH, Germany, in the form of a granulate of amorphous cycloolefin copolymer Topas®8007 (density 1.02 g/cm^3, norbornene content ca. 65 wt %, $T_g \sim 78$ °C).

2.1.2. Additives

Three additives were used: Synthetic phenolic antioxidant Irganox®1010 (Irg1010; supplied by Sigma Aldrich, Czech Republic), bio-based phenolic antioxidant α-Tocopherol (α-Toc; supplied by Signa Aldrich, Czech Republic), that is the most active component of vitamin E, and spin trapping agent 2,4,6-Tri-*tert*-butylnitrosobenzene (TTBNB; supplied by TCI–UK, Tokyo Chemical Industry, UK Ltd., Oxford, United Kingdom). The molecular structure of the additives denoted as Irg1010, α-Toc and TTBNB is presented in Scheme 1.

2.2. Preparation of polymer plaques

HDPE and COC plaques were prepared by standard melt-mixing followed by compression molding; the investigated additives were added during the melt-mixing step. UHMWPE could not be melt-mixed due to its extremely high molecular weight and viscosity, and so it was dry-mixed with the investigated additives and compression-molded at higher temperature and pressure.

HDPE powder and COC granulate were first homogenized by melt-mixing in the W 50 EH chamber of a twin-screw laboratory mixer (Brabender Plasti-Corder; Germany). HDPE samples were processed at 170 °C and 60 rpm for 8 min. After removing the material from the mixer chamber, 6 mm thick plaques 135 × 45 mm were compression-molded in a laboratory hot press at 180 °C for 1 min under 50 kN for deaeration plus another 2 min under 100 kN followed by water cooling to 70 °C for ca 15 min under 100 kN. COC samples were prepared by the same procedure, differing by the processing temperatures. The chamber temperature for the COC samples was set at 190 °C and the initial hot press temperature was set at 200 °C. The crystallinity of HDPE samples after processing was ~50 %; COC is an amorphous polymer.

The UHMWPE's plaques were prepared by the compression molding. The UHWMPE powder was dry-mixed with additives and filled into the 6 mm thick frame, which was covered with aluminum foil and a metal plate from each side. The covered frame was put into the hot press pre-heated at 230 °C for 5 min. Then the pressure was increased gradually, with a step of 25 kN up to 225 kN. At each step, the sample was left to equilibrate for 2.5 min. Finally, the hot press was cooled with water to standard laboratory temperature. The crystallinity of UHMWPE samples after processing was ~40 %.

A total of eighteen samples in the form of 6 mm thick plaques were prepared. Twelve of the prepared samples were subjected to WOM photooxidation (Section 2.3, Table 1). Six of the prepared samples were

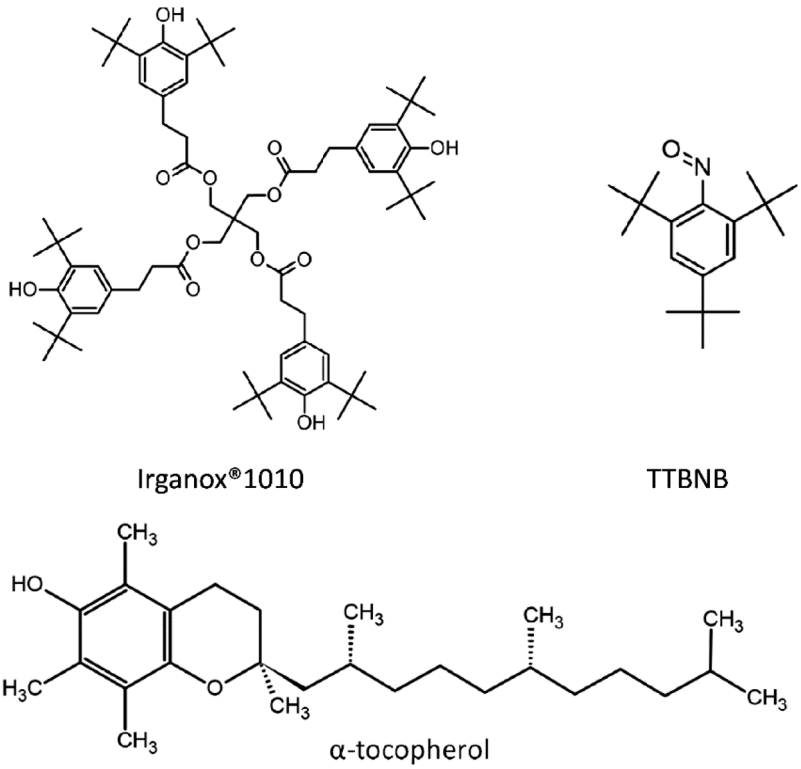

Scheme 1. Molecular structure of investigated stabilizers (Irganox®1010 and α-Tocopherol) and spin trapping agent (2,4,6-Tri-*tert*-butylnitrosobenzene; TTBNB).

Table 1
List of samples subjected to WOM aging.

Sample	Composition			
	Polymer	TTBNB (%)	αToc (%)	Irg1010 (%)
HDPE/0	HDPE	0	0	0
HDPE/TTBNB	HDPE	0.25	0	0
HDPE/α-Toc	HDPE	0	0.5	0
HDPE/ α-Toc /TTBNB	HDPE	0.25	0.5	0
HDPE/Irg1010	HDPE	0	0	0.5
HDPE/Irg1010/TTBNB	HDPE	0.25	0	0.5
COC/0	COC	0	0	0
COC/TTBNB	COC	0.25	0	0
COC/ α-Toc	COC	0	0.5	0
COC/ α-Toc /TTBNB	COC	0.25	0.5	0
COC/Irg1010	COC	0	0	0.5
COC/Irg1010/TTBNB	COC	0.25	0	0.5

subjected to e-beam irradiation (Section 2.4, Table 2).

2.3. Accelerated photooxidation of the plaques

The plaques were exposed to accelerated photooxidation in an Atlas Ci 3000+ Weather-Ometer (WOM; Atlas, USA) under the following conditions: filtered Xenon light wavelength bandpass 295–800 nm (inner and outer filter combination Type S Boro/Type S Boro), spectral irradiance 0.5 $Wm^{-2}nm^{-1}$ at 340 nm, black panel temperature (bpt) 60 °C, dry bulb temperature (dbt) 30 °C, RH 20 %. The plaques were irradiated for the overall net exposure of more than 50 days divided into periods of variable length in dependence on the development of the processes followed. The radiation falls on the front surface of the plaque, penetrates the plaque, and reaches its back surface. At the end of each period the plaques were removed from WOM and cylindrical samples of diameter ~3 mm assigned for ESR and ESRI measurements were bored out from the plaques in the direction perpendicular to their surface. ESR, ESRI, IR and MH measurements were performed as described below. The plaques were stored in the dark at ~10 °C for the time between the periods of WOM exposure. The complete list of samples subjected to accelerated photooxidation is given in Table 1.

Table 2
List of samples subjected to e-beam irradiation.

Sample	Composition Polymer	αToc (%)
HDPE/0	HDPE	0
HDPE/α-Toc	HDPE	0.5
UHMWPE/0	UHMWPE	0
UHMWPE/ α-Toc	UHMWPE	0.5
COC/0	COC	0
COC/α-Toc	COC	0.5

2.4. e-beam irradiation

The plaques were exposed to the electron beam using an electron beam accelerator ELV-2 (Budker Institute of Nuclear Physics, Novosibirsk, Russia) at the Leibniz Institute of Polymer Research Dresden (IPF Dresden e.V.), Germany [29,30]. The electron beam irradiation was carried out in the air, using 1.5 MeV electron energy and an electron current of 4 mA. Application of high dose rates (> 25 kGy/min) should minimize oxidation during the irradiation process [31,32]. All samples were irradiated under the same condition, using an irradiation dose of 100 kGy which was applied in 25 kGy steps. The complete list of samples subjected to e-beam irradiation is given in Table 2.

2.5. Electron spin resonance

ESR and 1D ESRI experiments were performed using a commercial Bruker ELEXSYS E-540 X-band spectrometer equipped with a pair of eight-shaped Lewis gradient coils that are able to produce a vertical magnetic field gradient perpendicular to the external magnetic field. The cylindrical samples were positioned vertically in the cavity of the

spectrometer, parallel to the direction of the magnetic field gradient. ESR spectra without magnetic field gradient and projections at magnetic field gradient 110 G/cm were measured at 298 K and microwave power output 6 mW using 100 kHz magnetic modulation of amplitude 2 G Concentration profiles of radicals in the samples along the axes of the cylinders coinciding with the direction of radiation incident on the plaques were determined by application suitable deconvolution procedure on 1D ESRI data [33].

2.6. Infrared and Raman microspectroscopy

2.6.1. HDPE polymer: FTIR line scans

Infrared spectra (IR) were measured using an IR microspectrometer (Thermo Nicolet 6700 with an FTIR microscope Continuum, equipped with the MCT detector). Slices of the polymer plaque ~200 μm thick were cut along the direction of the incident light (perpendicular to the surface of the plaque) from inside the plaque with a sledge microtome (Meopta; Czech Republic). The infrared spectra of the microtomed slices were measured using a transmission mode by accumulation of 4 scans with a resolution of 4 cm^{-1}. The spectra were measured as linear scans, i.e. the measurement for each sample was made in a line along the direction perpendicular to the surface of the plaque. The distance between the individual measurements in the line was 200 μm.

For HDPE and UHMWPE plaques, several IR indexes were calculated from each spectrum: The oxidation index (OI; proportional to the local oxidative degradation), crystallinity index (CI; proportional to the local volume fraction of crystalline phase), *trans*-vinylene index (VI; proportional to the absorbed radiation dose), stabilizer index (SI, proportional to the concentration of selected stabilizer group in given location) and spin-trap index (TI, proportional to the concentration of TTBNB). The TI index calculated only for the HDPE/TTBNB and UHMWPE/TTBNB samples due to the overlap of the markers band for the calculation of SI and TI.

The calculation of OI, CI and VI indexes (Eqs. (1)–(3)) was common for all HDPE and UHMWPE plaques, regardless of the stabilizer:

$$\mathrm{OI} = \frac{A_{1720}}{A_{1370}} \tag{1}$$

$$\mathrm{CI} = \frac{A_{1897}/A_{1303}}{A_{1897}/A_{1303} + 0.3} \tag{2}$$

$$\mathrm{VI} = \frac{A_{965}}{A_{1370}} \tag{3}$$

The oxidation index (OI; Eq. (1)) was determined as the ratio of the carbonyl band area (1720 cm^{-1}) to the methylene band area (1370 cm^{-1}) [34,35]. The crystallinity index (CI; Eq. (2)) was calculated using the formula CI ≈ CA/(CA + 0.3), where CA is the ratio of the area of the band at 1897 cm^{-1} (assigned to the PE crystalline phase) to the area of the band at 1303 cm^{-1} (assigned to the PE amorphous phase) [36,37]. The *trans*-vinylene index was determined as the ratio of the carbonyl (*trans*-vinylene) group (965 cm^{-1}) to the area of the reference peak corresponding to vibrations of both amorphous and crystalline parts of virgin polyethylene [32,38,39].

The calculation of the stabilizer index (SI) was specific for each selected stabilizer. Due to different chemical composition of the stabilizes, we have to detect each stabilizer by means of different vibration band and, as a result, each stabilizer had its own definition of SI.

For HDPE/α-Toc and UHMWPE/α-Toc the stabilizer index (SI (α-Toc), Eq. (3)) was defined as the ratio of C-O stretching vibration of the phenol group (1210 cm^{-1}) to the area of the methylene band vibration (1370 cm^{-1}). Calculation of the SI(α-Toc) is based on the study of Costa [34] and was experimentally proved in our previous works [1,2].

$$\mathrm{SI}(\alpha - \mathrm{Toc}) = \frac{A_{1210}}{A_{1370}} \cdot 10 \tag{4}$$

For HDPE/Irg1010 and UHMWPE/Irg1010 mixtures, the stabilizer index ($SI_{Irg1010}$, Eq. (4)) was calculated as the ratio of the integral intensity of the 1150 cm^{-1} band related to the methylene band vibration area (1370 cm^{-1}). The band at 1150 cm^{-1} was assigned to the C-O-C vibration of Irg1010. This calculation has already been successfully applied in our previous studies [2]:

$$\mathrm{SI}(\mathrm{Irg1010}) = \frac{A_{1150}}{A_{1370}} \tag{5}$$

For the HDPE/TTBNB and UHMWPE/TTBNB mixtures, the TTBNB index denoted as TI (instead of SI, because a spin-trapping agent is not a stabilizer) was determined. Evaluation of TI was experimentally proved in our previous work [3]. TI index (Eq. (5)) was evaluated as the ratio of the integral intensity of the C—O band at 1250 cm^{-1} to the methylene vibration area (1370 cm^{-1}). The intensity of the 1250 cm-1 band is very low and this band is clearly visible and well identifiable only in the pure HDPE matrix. Due to its low intensity, the characteristic peak ratio defining TI index was multiplied by 30:

$$\mathrm{TI} = \frac{A_{1250}}{A_{1370}} \cdot 30 \tag{6}$$

As the OI, CI and SI or TI indexes were measured as linear scans their values could be plotted as a function of distance, *L*, from the exposed surface. Such plots are called OI, CI, SI and TI profiles in the following text. The OI, CI, SI and TI profiles represented the main output from IR analyses of HDPE mixtures. Analogous calculations of IR indexes were described also in our previous papers [1–3,39].

2.6.2. COC copolymer: ATR spectra from surfaces

Preparation of the 200 μm thick slices of the COC copolymer plaque has not been possible due to the stiffness and brittleness of the material. For this reason, the COC samples were characterized in their bulk form using Attenuated-Total-Reflectance (ATR) FTIR spectroscopy. The ATR spectra were measured from their exposed and back surface. The spectra were recorded on Thermo Scientific™ Nicolet™ iN10 Infrared Microscope equipped with an LN-cooled MCT detector at a resolution of 4 cm^{-1} using a Ge single reflection ATR crystal. Each spectrum was obtained as an average of 256 scans. A spectrum of water vapor was subtracted from the acquired spectrum, which was then processed by baseline and ATR corrections using the OMNIC software. The spectra were evaluated qualitatively. The semi-quantitative nature of the ATR technique and the fact that COC spectra contained a higher number of overlapping absorption bands than PE spectra made impossible calculation of indexes or profiles like in the case of transmission IR spectra of PE samples and prevented their quantitative interpretation.

2.7. Micromechanical properties

Micromechanical properties were measured with instrumented microindentation hardness tester (MCT tester; CSM, Switzerland). The microindentation hardness testing (MHI) experiments were carried out using a Vickers method: a diamond square pyramid (with an angle between non-adjacent faces 136°) was forced against the flat surface of a specimen. The micromechanical properties were deduced from the loading force, which was measured as s function of penetration depth. The surface of prepared plaques after the compression molding was flat enough to provide MHI measurement directly from the surface.

MHI was used for the characterization of COC and HDPE plaques both on the WOM exposed and back surfaces. For each measured surface, at least 25 independent measurements/indentations were made and the final results were averaged. The parameters of MHI measurements were as follows: loading force 500 mN, dwell time (time of maximal load) 60 s, and linear loading and unloading rates 12 000 mN/

min.

The evaluated micromechanical properties were Martens hardness (H_M) also referred as universal hardness, indentation hardness (H_{IT}) proportional to macroscopic yield stress, indentation modulus (E_{IT}) proportional to macroscopic elastic modulus, indentation creep (C_{IT}) related to the macroscopic creep, and elastic part of the indentation work (η_{IT}) defined as ratio of elastic deformation to total deformation. The calculations of H_{IT}, E_{IT}, C_{IT} and n_{IT} were based on the theory of Oliver and Pharr [40]: The exact definitions of above-listed micromechanical properties can be found in suitable reviews or textbooks dealing with micro- and/or nanoindentation [41,42]; a more detailed description of the MHI experiments also in our recent studies [43–45].

2.8. Light and electron microscopy

Morphological changes of selected plaques after accelerated photooxidation were visualized by light microscopy (LM)). LM micrographs were obtained with a light microscope Nikon Eclipse 80i (Nikon, Japan) equipped with a digital camera ProgRes CT3 (Jenoptik, Germany). The specimen surfaces were observed in reflected light. The color changes of the exposed surface were observed at stereo-microscope SMZ-2T (Nikon, Czech Republic).

2.9. Data processing

ESR data were processed and plotted in a standard way, like in our previous work [1–3]. IR profiles were calculated with our software MPINT [39]. Statistical evaluation of the results, namely the quantification of the correlations between local crystallinity and local mechanical properties, was made by means of Python programming language and its freeware packages for data processing and statistics [46]. More details about statistics, especially about quantitative evaluation of correlations, can be found in suitable textbooks of statistics [47].

3. Results

All samples (HDPE, COC and UHMWPE with various stabilizers) were prepared in the form of 6 mm thick plaques. Twelve samples (Table 1) were subjected to non-ionizing radiation (photooxidation) and six samples (Table 2) were subjected to ionizing radiation (e-beam irradiation). The radicals and oxidation products were monitored as a function of distance from the exposed surface by ESR spectroscopy (Sections 3.1 and 3.2) and IR microspectroscopy combined with characterization of local mechanical properties (Sections 3.3 and 3.4), respectively.

3.1. ESR spectroscopy of photo-oxidized samples

3.1.1. HDPE samples

ESR spectrum created by superposition of spectra of anilino-type (I B) and nitroxide-type (II B) adducts of polymer alkyl radicals to TTBNB described by Qu et al. [14] has been observed in the HDPE samples containing this spin trap (HDPE/TTBNB, HDPE/α-Toc/TTBNB, HDPE/Irg1010/TTBNB) before WOM exposure (Fig. 1 left column). The same spectrum was observed and discussed previously [8] in HDPE/TTBNB samples containing phenolic stabilizer (+)-Catechin hydrate (CAT) as the second additive (Fig. 2). No detectable radicals have been identified before WOM exposure in the HDPE samples at the absence of the spin trap TTBNB (additive free HDPE, HDPE/α-Toc, HDPE/Irg1010) where only unresolved lines of low intensity have been observed. A rapid decrease of concentration of adducts together with their transformation has been observed after WOM exposure (3, 10, 20,

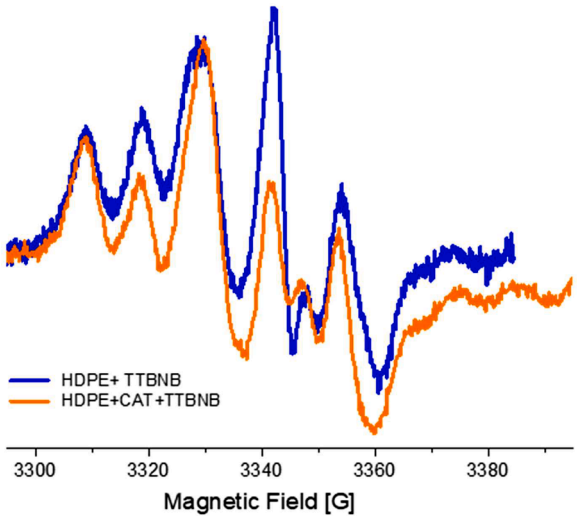

Fig. 2. ESR spectra of spin adducts of HDPE alkyl radicals with TTBNB measured before WOM exposure in HDPE+TTBNB sample (blue line) and in the HDPE+CAT+TTBNB sample (orange line); the later spectrum is taken over from the Ref. [8].

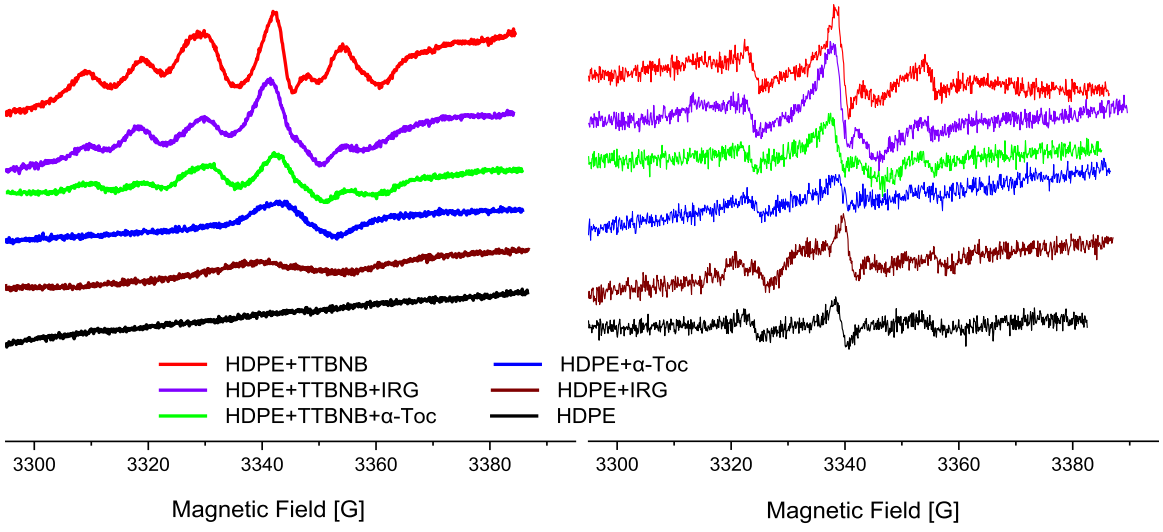

Fig. 1. ESR spectra of HDPE samples measured before WOM exposure (left) and after 10 days of WOM exposure (right).

30 days). Similar rapidly decreasing weak ESR signals have been observed in the rest of the samples as well (Fig. 1 right column). Spectra measured after 10 days of WOM are presented as an example in Fig. 1 right column. Even weaker spectra have been measured after longer WOM exposure.

3.1.2. COC samples

Before WOM exposure weak ESR spectra of α-tocopheroxyl radical α-Toc$^{\bullet}$ have been observed in the COC samples containing α-Toc and spectra of immobilized adducts of some radicals to TTBNB (immobilized nitroxides) have been observed in the COC samples containing TTBNB (Fig. 3), no signals have been detected in the rest of COC samples (plain COC and COC + Irg1010).

After WOM exposure (3, 10, 20, 30 days) broad doublet has been observed in cylindrical samples bored out from the additive free COC plaques and COC/Irg1010, COC/TTBNB and COC/TTBNB/Irg1010 plaques (Fig. 4, right column). This doublet was ascribed [7] to relatively stable polymer alkyl radicals considered by Nakade et al. [10,16] as intermediates generated during the photodegradation of ethylene-norbornene random copolymers. ESRI has shown a practically homogeneous distribution of the polymer alkyl radicals in the COC/Irg1010 sample and a similar distribution with a slightly higher concentration of radicals in the middle of the plate in the COC/Irg1010/TTBNB sample that are the samples with the highest concentrations of polymer alkyl radicals observed (Fig. 5). A high concentration of stable α-tocopheroxyl radicals α-Toc$^{\bullet}$ has been observed after WOM exposure in the samples containing α-Toc, particularly in the sample COC/α-Toc and somewhat lower concentration in the sample COC/α-Toc/ TTBNB (Fig. 4, left column). Heterogeneous distribution of α-tocopheroxyl radicals showing a higher concentration of the radicals in both surface layers when comparing with internal layers, in the irradiated surface layer in particular, has been observed in the sample COC/α-Toc (Fig. 5) by ESRI. ESRI. Increasing of WOM exposure time above 10 days did not affect the spectra and concentration of polymer alkyl and α-tocopheroxyl radicals in the samples. The spectra measured after 20 days of WOM exposure are shown as an illustrative example.

3.2. ESR spectroscopy of e-beam irradiated samples

3.2.1. HDPE and UHMWPE samples

No significant ESR signals have been observed in the HDPE and UHMWPE samples before irradiation by an electron beam. ESR spectrum of the mixture of polymer allyl and alkyl radicals has been observed shortly after irradiation (after storage for several hours) in the neat HDPE and UHMWPE samples. A spectrum of allyl radical (7 equidistant lines a^{H}=13.5 G, g = 2.0016) described by Jahan [11] prevails in the mixture (Fig. 6). Ohnishi et al. [12,13] have found that in UHMWPE allyl radicals are generated by medium doses of electron radiation (100–1000 kGy) while alkyl radicals characterized by different type of ESR spectrum are generated by low doses of electron radiation (<10 kGy). The concentration of the radicals decreased with storage time. They have been subjected to transformation reactions including oxidation processes resulting in the generation of transient secondary radicals, e.g. peroxyls and alkoxyls, and a variety of products. Observed ESR spectra of secondary radical mixture could not be analyzed (Fig. 6). After irradiation of UHMPWE and HDPE samples stabilized with 0.5 wt.% of α-Toc by electron beam, no distinct spectra of polymer allyl or alkyl radicals could be detected, but we observed the spectra of a radical mixture similar to the spectra of the additive-free samples after several days of storage (Fig. 7). This suggested that α-Toc speeded up the transformation of the primary polymer alkyl and allyl radicals generated in UHMPWE and HDPE during e-beam irradiation. The radicals were transformed to the mixture of secondary radicals (like in the case of additive-free polymers). Therefore, the significantly higher transformation rate prevented us from observing ESR spectra of the original alkyl and allyl radicals and we observed only the final mixture of secondary radicals.

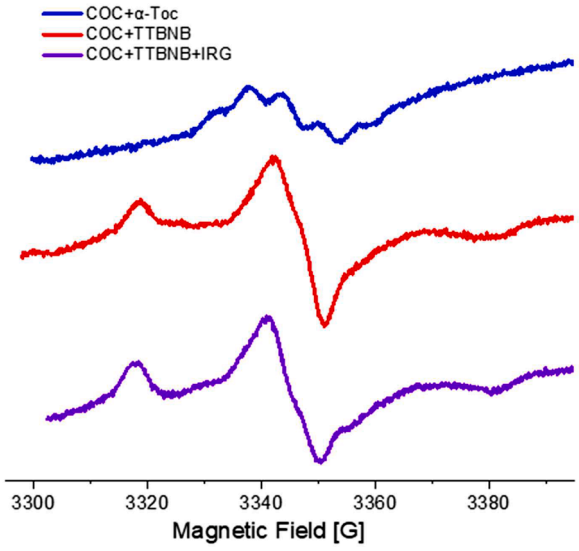

Fig. 3. ESR spectra of COC samples before WOM exposure.

3.2.2. COC samples

Rather weak ESR spectra of α-tocopheroxyl radical α-Toc$^{\bullet}$ have been observed in the COC samples containing α-Toc before irradiation by an electron beam. The broad line corresponding presumably to a mixture of polymer radicals, the concentration of which decreased with storage time, has been observed in the ESR spectrum of additive free COC sample irradiated by ionizing radiation (Fig. 8, left column). ESR spectrum of stable α-tocopheroxyl radicals α-Toc$^{\bullet}$ has been observed in the COC samples stabilized with 0.5 wt.% of α-Toc after the same treatment (Fig. 8, right column). Heterogeneous distribution of α-tocopheroxyl radicals in the sample showing a higher concentration of radicals in both surface layers when compared with internal layers (Fig. 5) has been found by ESRI. The concentration of α-tocopheroxyl radicals independent of storage time and representing roughly half of the concentration of α-tocopheroxyl radicals α-Toc$^{\bullet}$ generated in the similar samples by non-ionizing radiation (WOM) has been found. No polymer radicals have been detected in the COC samples stabilized with α-Toc.

3.3. Structure and micromechanical properties of photo-oxidized samples

3.3.1. HDPE samples

Fig. 9 summarizes the key results of IR microspectroscopy for HDPE samples. The upper row displays the samples before WOM exposure. These samples suffered only from thermo-mechanical oxidative degradation (also referred to as thermooxidation), i.e. from the elevated temperatures during melt mixing (as described in Section 2.2). The lower rows show samples during WOM exposure, i.e. after both thermooxidation and photooxidation (Sections 2.2. and 2.3).

Before WOM exposure (Fig. 9, the upper row), the neat HDPE sample had already been partially degraded due to thermooxidation (as evidenced by the non-zero values of OI), while the samples containing spin trap (HDPE/TTBNB), α-Tocopherol (HDPE/α-Toc) and their combination (HDPE/α-Toc/TTBNB) were stable (low values of OI for HDPE/TTBNB and negligible OI's for all other samples). The samples containing Irg1010 stabilizer were protected against thermooxidative degradation as well. The non-zero values of OI came from the carbonyl groups of Irg1010 itself. This is proved by the plots displaying OI profiles of HDPE/Irg1010 and HDPE/Irg1010/TTBNB sample at higher WOM exposure times (the two rightmost columns of Fig. 9), in which the OI values in the center of the samples (i.e. in the regions non-influenced by the photooxidative degradation), remained constant.

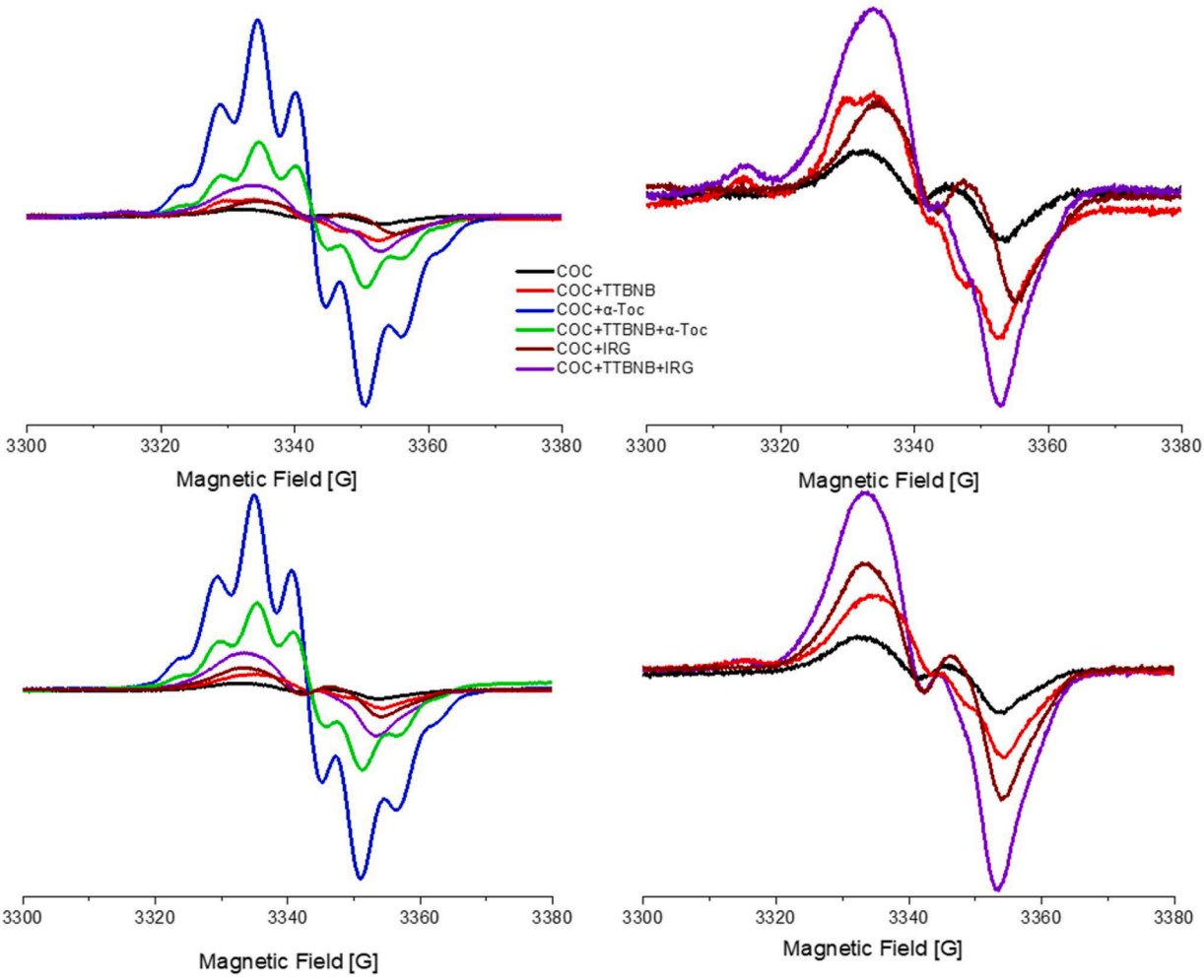

Fig. 4. ESR spectra of all COC samples studied measured (left column) after 3 days (upper row) and after 20 days (bottom row) of WOM exposure and the spectra of the samples without α-Toc additive at six times larger vertical scale (right column).

After the WOM exposure (Fig. 9, the second row and below) the differences among the samples increased. The non-stabilized (neat) HDPE/0 sample exhibited medium oxidative degradation at the beginning of WOM and very strong oxidation at the end of WOM aging at both edges (exposed and back). The HDPE/TTBNB sample showed slower oxidative degradation than HDPE/0: the oxidation at the beginning of WOM was lower and the oxidation at the opposite, non-exposed edge was the lowest of all samples. The samples with the phenolic stabilizers (HDPE/α-Toc and HDPE/Irg1010) exhibited higher oxidative degradation than HDPE/0 at the exposed edge (the difference was the highest at the beginning of WOM exposure), while the oxidation at the back edge was somewhat different – the maximum OI values were lower than those in HDPE/0, but the oxidation occurred deeper inside the specimen. The behavior of the two samples containing a phenolic stabilizer with the spin trap (HDPE/α-Toc/TTBNB and HDPE/Irg1010/TTBNB) was in between the behavior of the sample containing just the spin trap (HDPE/TTBNB) and the two samples containing just the stabilizers (HDPE/α-Toc and HDPE/Irg1010) – the TTBNB slightly mitigated the prooxidant activity of α-Toc and Irg1010.

In the previous paragraphs, we described the oxidative degradation, characterized by OI profiles. The remaining three profiles (CI-, TI- and SI-profiles) yielded useful additional information concerning the local changes of molecular and supramolecular structure of the samples. The CI-profiles were almost the same and quite constant in all samples. They just slightly increased at the edges of highly oxidized samples, because oxidative degradation causes chain scissions followed by cold crystallization, as described elsewhere [2,32]. The TI-profiles were constant in the whole volume of all samples regardless of WOM exposure time (in Fig. 9, TI is shown only for HDPE/TTBNB samples), which confirmed the homogeneous distribution of TTBNB in the samples. As for SI-profiles, even a modest oxidative degradation (i.e. a modest increase in OI) caused a notable decrease SI, evidencing that the stabilizer took part in the chemical changes of the specimen. A notable exception was sample HDPE/α-Toc/TTBNB, in which the whole TI profile decreased to almost zero at the very beginning after thermooxidation, even before WOM exposure. This indicated that α-Toc active group (aryl-OH; Section 2.6.1, Eq. (4)), from which the TI is determined, interacted intensively with TTBNB during the melt-mixing.

Figs. 10 and 11 show 2D spatial evolution of IR spectra for HDPE/0 and HDPE/α-Toc samples before and after 30 days of WOM exposure. In comparison with IR peak profiles (Fig. 9), the 2D spatial evolutions display additional IR peaks and reveal further details of the structure changes. For the investigated HDPE samples, we recognize three important regions connected with the oxidation and scission of polyethylene chains:

- Region of oxidation products (1600–1850 cm^{-1}): The decomposition and detailed discussion of these oxidation-products-related peaks can be found elsewhere [1,48]. Briefly, the peaks around 1720 cm^{-1} are attributed to ketones, the peaks around 1740 cm^{-1} are attributed to esters, and the peak around 1640 cm^{-1} is attributed to C=C stretch vibrations in the vicinity of hydroperoxides.

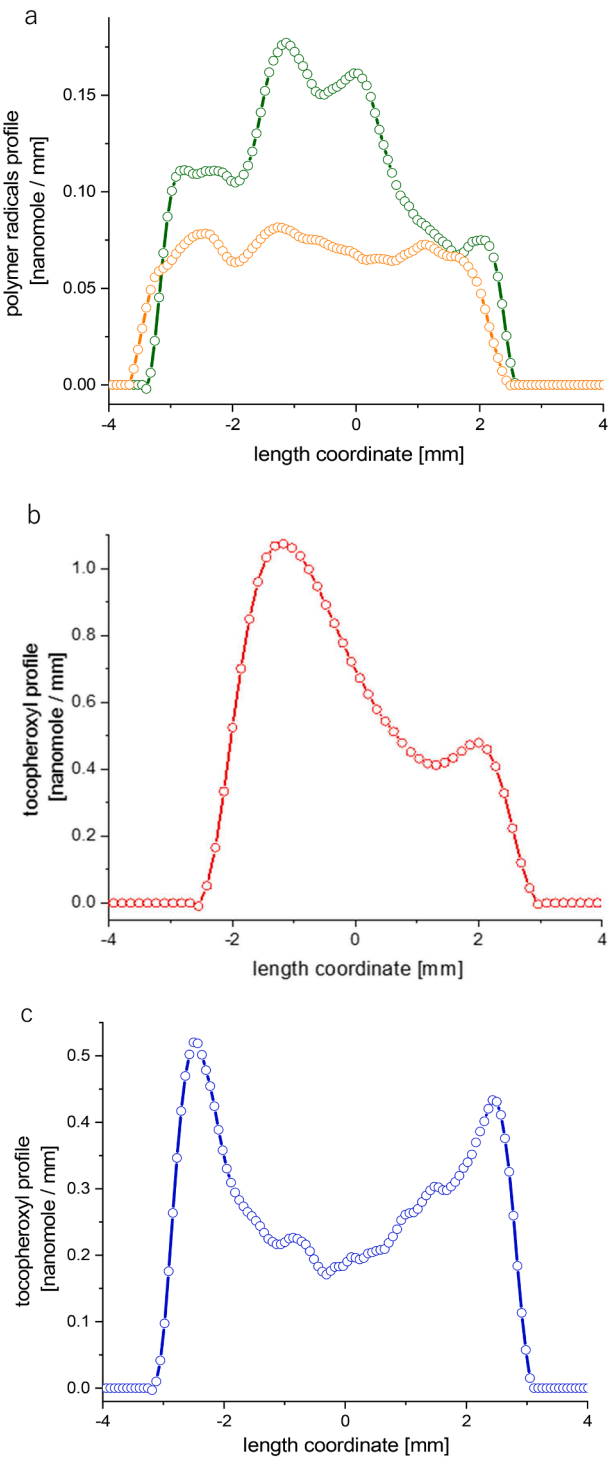

Fig. 5. Concentration profiles of radicals inside plates along the axis perpendicular to their surface (parallel to the direction of irradiation); (a) polymer radicals in the plate made of COC copolymer stabilized with 0.50 wt% of Irg1010 (orange) and with 0.50 wt% of Irg1010 + 0.25 wt % of TTBNB (green) after 30 day's WOM exposure and 8 month's storage (~ 50 % of radicals survived in both samples); (b) tocopheroxyl radicals in the plate made of COC copolymer stabilized with 0.50 wt% of α-Toc after 30 day's WOM exposure and 8 month's storage (64 % of radicals survived, red); (c) tocopheroxyl radicals in the plate made of COC copolymer stabilized with 0.50 wt% of α-Toc irradiated by ionizing radiation after 8 month's storage (70 % of radicals survived, blue).

- Region of unsaturated C=C bonds (900–1000 cm^{-1}): This region contains three weak peaks at 909, 965 and 991 cm^{-1}. Two of them correspond to terminal C=C bond (terminal vinyl; 909 and 991 cm^{-1}) and the last corresponds to medial C=C bod (in-chain trans-vinylene; 965 cm^{-1}). The terminal C=C bonds appear as a result of chain scissions [49].
- Region of α-Tocopherol specific bonds (1210–1270 cm^{-1}): There are two peaks specific of α-Toc, which are not observed at neat HDPE. The band at 1211 cm^{-1} corresponds to C-O stretching of the phenol group and the band at 1263 cm^{-1} corresponds to aryl-O-alkyl ether group (see Scheme 1 and Refs. [1,50].

All the above-mentioned important peaks are denoted in both Figs. 10 and 11. The dominating change in the non-stabilized HDPE/0 sample (Fig.10) after irradiation was the increase in terminal vinyl double bonds at both surfaces (compare peaks 909 and 991 cm^{-1} in Figs. 10a and c) and, above all, the steep increase in oxidation products close to the exposed surface (peaks around 1720 cm^{-1}). The increased concentration of terminal vinyl C=C bonds at both surfaces was a sign of chain scissions that indicated a polymer degradation. This correlated with the increase of oxidation products close to both surfaces. Moreover, the 2D map of oxidation products (Fig. 10d) evidenced that the composition of the oxidation products at the exposed surface (mostly ketones with the maximum around 1720 cm^{-1}) was somewhat different from the composition of the oxidation products at the back surface (both ketones with the maximum around 1715 cm^{-1} and esters around 1740 cm^{-1} or higher). HDPE/α-Toc sample (Fig. 11) followed the same general trends (increase in terminal double bonds and oxidation products at both exposed and back surface), but several differences could be identified. At first, the ratios between double bond-related peaks were different and the band corresponding to in-chain trans-vinylene group (965 cm^{-1}) showed negligible intensity (Fig. 11a and c). At second, both the concentration and composition of oxidation products at the exposed and back surfaces differed more than in the case of HDPE/0 – the total concentration of oxidation products HDPE/α-Toc was higher than in HDPE/0 at the exposed surface and lower at the back surface (Fig. 11c and d). Moreover, the oxidation at the back surface penetrated to higher depth in HDPE/α-Toc than in HDPE/0 (which agrees with the corresponding OI profiles in Fig. 9). These results (i) confirmed the prooxidant activity of α-Toc and (ii) indicated that the photooxidative degradation process in HDPE/0 and HDPE/α-Toc was influenced by the presence of the stabilizer.

Fig. 12 illustrates how oxidative degradation influences the local mechanical properties of all HDPE samples. As mentioned above, the oxidative degradation of semicrystalline polymers leads to chain scissions, cold crystallization and an increase in overall crystallinity [32,51]. The stiffness-related properties of semicrystalline polymers (such as elastic modulus, yield strength and hardness) are directly proportional to crystallinity [35,37,45,52]. During photooxidation, the oxidative degradation and crystallinity at the exposed edge of all investigated samples increased (Fig. 9), which resulted in an increase of all local stiffness-related micromechanical properties (Fig. 12). The fact that the two completely independent microscale methods – IR microspectroscopy and microindentation hardness testing – yielded compatible results can be regarded as an important confirmation of the reliability and reproducibility of our measurements.

3.3.2. *COC samples*

Fig. 13 summarizes the IR results for all investigated COC samples. The IR spectra of COC samples were measured by the ATR technique. The key advantage of ATR consisted in the fact that it did not require thin sections. For the stiff and brittle COC samples, the preparation of thin section was rather problematic. The ATR spectra of COC samples were measured for each sample at several locations on the exposed and back surfaces. Fig. 13 shows just representative spectra from the exposed surfaces (the spectra from the back surfaces showed basically the same

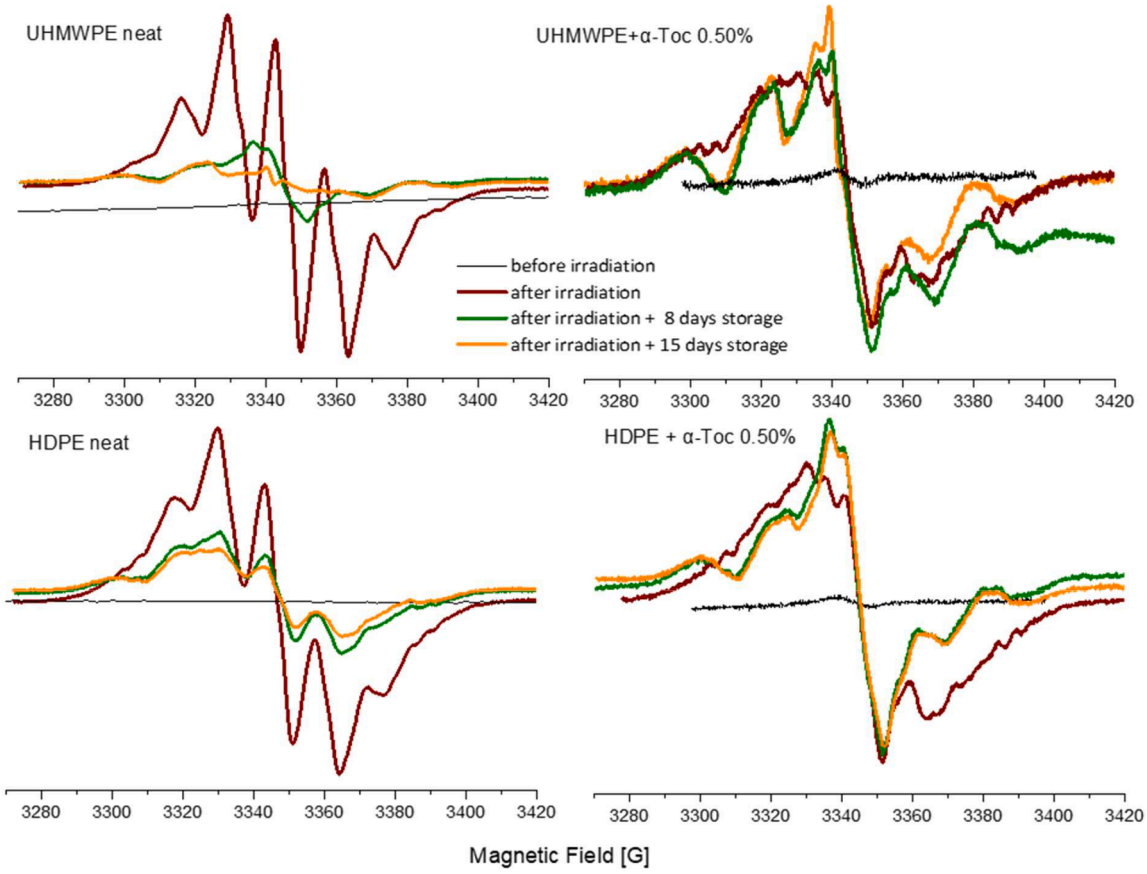

Fig. 6. ESR spectra of e-beam irradiated UHMWPE and HDPE samples neat and stabilized with 0.5 % α-Toc in dependence of storage time.

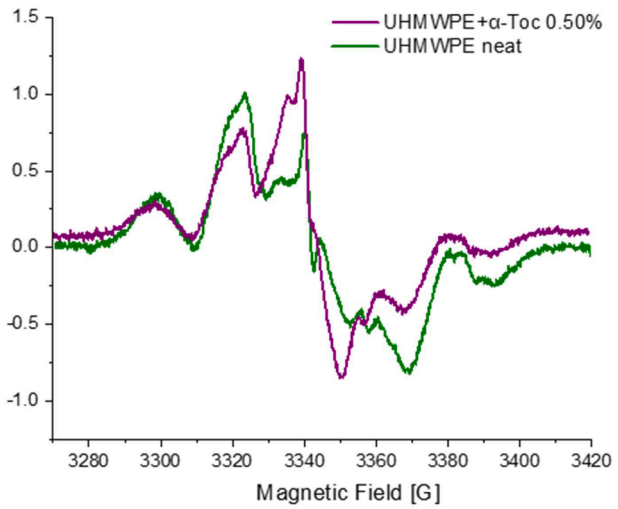

Fig. 7. Comparison of ESR spectra of radical mixtures observed in e-beam irradiated neat UHMWPE and UHMWPE stabilized with 0.5 % α-Toc samples both after 15 days' storage time.

trends, but the differences among various samples and WOM exposure times were less pronounced).

The ATR spectra of all COC samples were dominated by strong bands of aliphatic C-H stretching vibrations (2800–3000 cm^{-1}), while the other COC bands in the fingerprint region (below ca 1500 cm^{-1}) were weaker. The oxidative degradation of COC samples manifested itself by an absorption increase in the following three regions of ATR spectra: (i) the broad region 900–1300 cm^{-1}, corresponding to C–O stretching vibrations occurring in esters or ethers, (ii) the relatively narrow and sharp band around 1720 cm^{-1}, corresponding to the characteristic stretching vibration of C=O groups, and (iii) the broad band 3000–3600 cm^{-1}, corresponding to hydroxyl valence bond vibrations.

All COC samples were quite resistant to thermo-oxidative degradation during melt-mixing (in contrast to HDPE), as documented by negligible damage before WOM exposure (Fig. 13, the brightest curves at 0 d of WOM). Moreover, all COC samples exhibited fair stability during the first 20 days of WOM exposure (Fig. 13, intermediate curves at 20 d of WOM). However, at 50 days of WOM exposure, the degradation on the exposed surface was very high (Fig. 13, the darkest curves at 50 d of WOM). Neat COC sample (Fig. 13a) was the most stable. COC/TTBNB sample (Fig. 13b) documented that the TTBNB spin trap alone showed certain pro-oxidant activity. Both samples containing α-Toc (COC/α-Toc and COC/α-Toc/TTBNB; Fig. 13c and d) showed the highest oxidative degradation (note the steep increasing in the main oxidation peak around 1720 cm^{-1}), which evidenced strong prooxidant activity of α-Toc in COC. In contrast, both samples containing Irg1010 (COC/Irg1010 and COC/Irg1010/TTBNB; Fig. 13e and f) showed significantly lower oxidative degradation than neat COC, evidencing antioxidant activity of Irg1010 in COC. The sample with both Irg1010 and TTBNB (Fig. 13f) displayed somewhat higher oxidative damage, re-confirming that TTBNB acted as a prooxidant in COC systems (compare Fig. 13a vs. 13b and 13e vs. 13f).

Fig. 14 summarizes the main results of microscopic and micromechanical characterization of COC samples. The figure shows imprints of the indenter on the exposed surfaces of all investigated COC samples after 50 d of WOM exposure. The fact that the size of the imprint is more-or-less the same proved that the oxidative degradation had a negligible effect on micromechanical properties. This indicated that COC samples were resistant enough to both thermo-oxidative and photo-oxidative

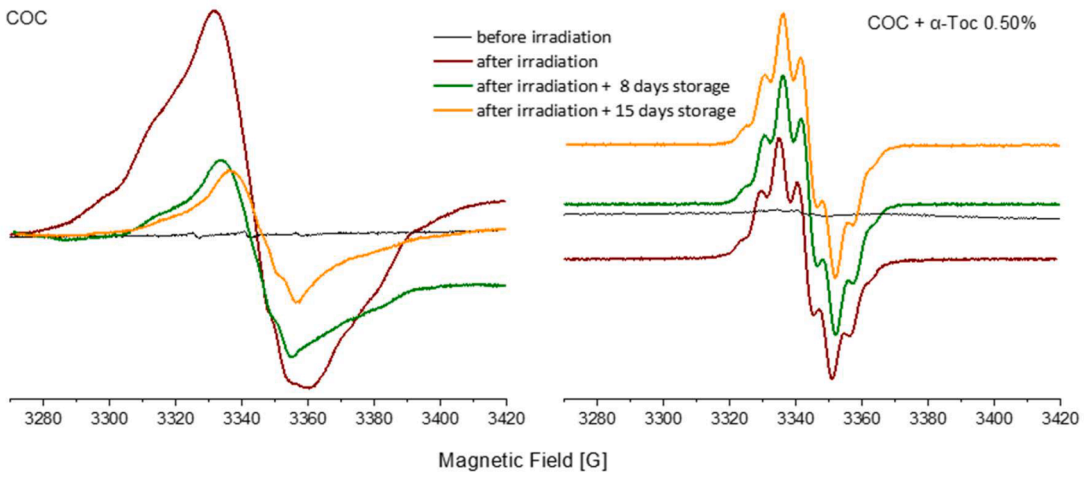

Fig. 8. ESR spectra of e-beam irradiated neat COC and COC + 0.5 % α-Toc samples after storage.

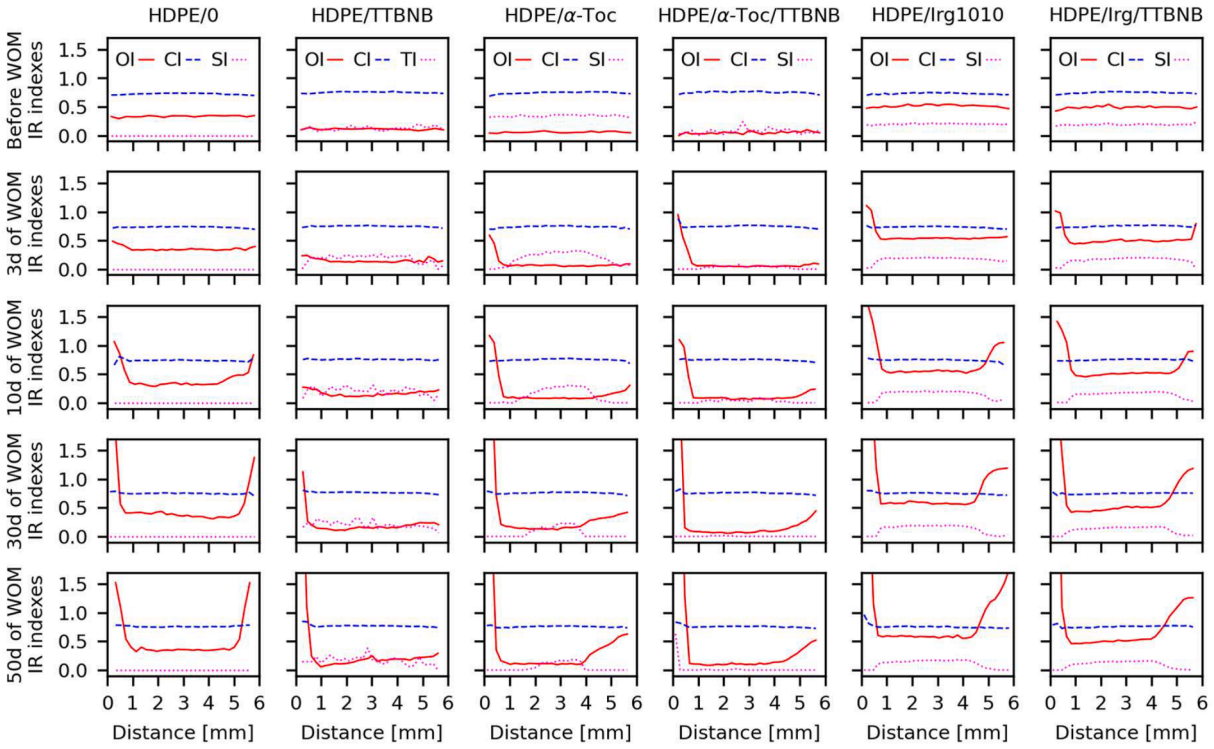

Fig. 9. IR analysis results for all PE samples with/without selected stabilizer (α-Toc, Irg1010) and/or spin-trapping agent (TTBNB). Samples are arranged in columns and name of each sample is on the top of the column. Each sample was characterized several WOM exposure times (rows from top to bottom: 0, 3, 10, 30 and 50 days). Every subplot displays profiles of oxidation index (OI; Eq. (1)), crystallinity index (CI; Eq. (2)), stabilizer index (SI; Eqs. (4) and (5)) and/or spin-trap index (TI; Eq. (6)).

degradation and, consequently, the damage occurred only at the very surface layer that was characterized by ATR measurements (Fig. 13 above). A full evaluation of MHI measurements on COC samples is given in Supplementary materials (Fig. S1). The long linear grooves on the COC sample surfaces in Fig. 14 come from the processing (we measured "as prepared" surfaces after melt-mixing and compression molding). Nevertheless, the observed microcracks correlated nicely with the ATR results: The most pronounced microcracks were observed for samples with TTBNB and α-Toc, which acted as pro-oxidants in COC samples (compare Figs. 13 and 14).

3.4. Structure and micromechanical properties of e-beam irradiated samples

3.4.1. HDPE and UHMWPE samples

Fig. 15 summarizes key structural changes of polyethylene polymers (HDPE and UHMWPE) after e-beam irradiation. The two polymers exhibited similar behavior regardless of the difference in their molecular mass (1×10^5 g/mol for HDPE and 4×10^6 g/mol for UHMWPE). We note that Fig. 15 shows trans-vinylene index (VI) instead of stabilizer index (SI) in the analogous Fig. 9. The reason is that the SI profiles are uninteresting here: Before the e-beam irradiation, the SI profiles were constant (as documented in the first row of Fig. 9), while the e-beam

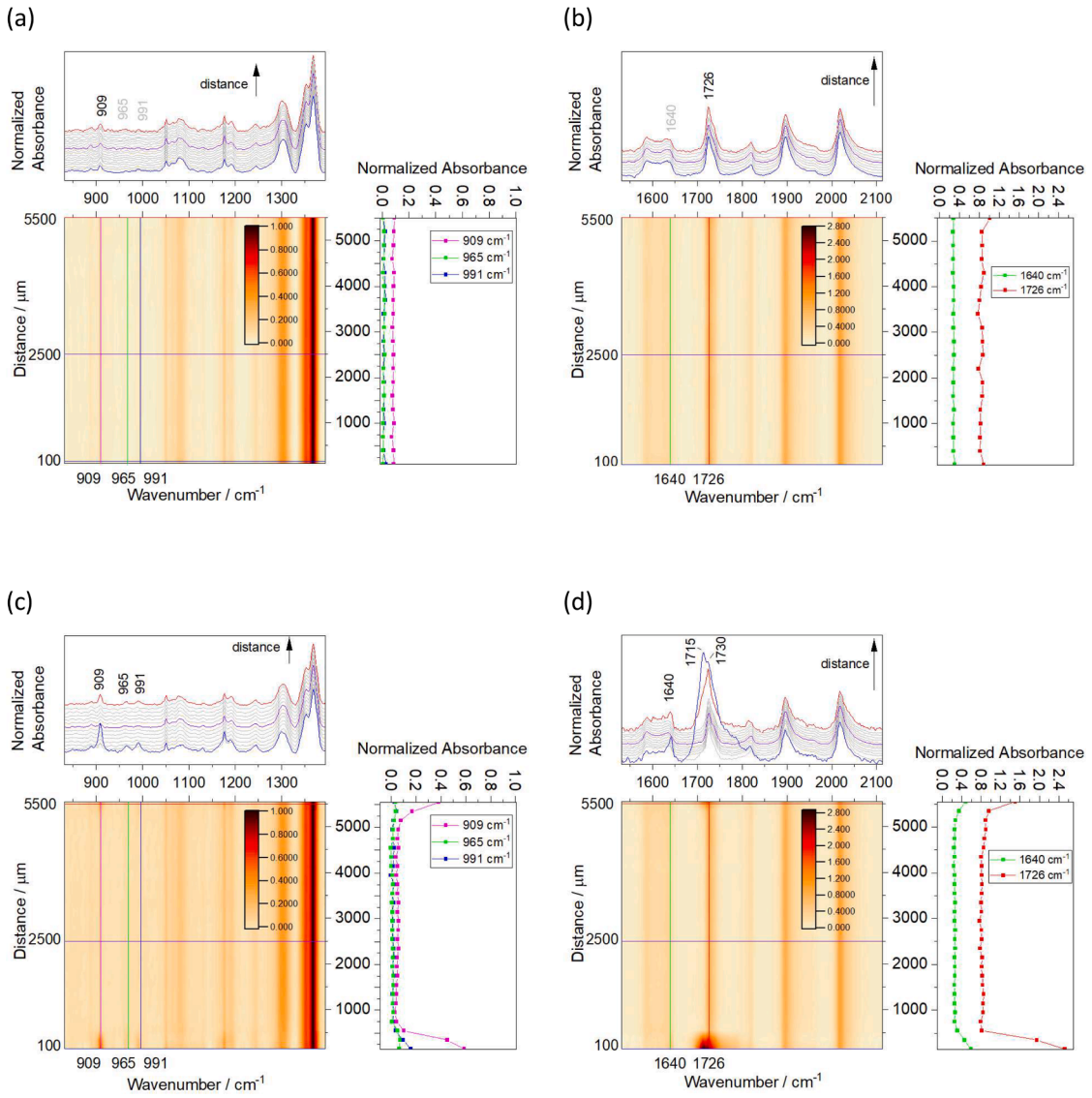

Fig. 10. 2D images of IR spectra as a function of distance from the exposed surface: (a, b) Spectra HDPE/0 sample before WOM exposure. (c, d) Spectra of HDPE/0 sample after 30 days of WOM exposure. Each of the four Figures (a–d) consists of a 2D-heatmap showing IR intensities, top plot showing a series of representative IR spectra, and left plot showing normalized absorbance of selected IR bands. All bands in the left Figures (a, c) and right Figures (b, d) were normalized to the same peak at 1380 cm^{-1} and 2020 cm^{-1}, respectively. The wavelengths of key peaks are marked in each image; the grey font indicates that given peak is either weak or missing.

irradiation resulted in the complete extinction of the phenol stretching vibration at 1210 cm^{-1} (as explained elsewhere [49]), which resulted in zero values of SI (as evident from Eq. (4)). This just documented that the high-energy electrons penetrated in the whole volume of the sample and the residual radicals immediately interacted with the active phenol group of α-Toc. On the other hand, the values of VI are quite interesting for us, because the formation of C=C bonds is one of the side reactions of e-beam-induced residual radicals with polyethylene [50].

Oxidative degradation in non-stabilized samples before e-beam irradiation was low (samples HDPE/0 and UHMWPE/0; OI profiles in the 1st row of Fig. 15). Slightly higher values of OI for HDPE/0 could be attributed to different preparation protocols (Section 2.2): the lower-viscosity HDPE powder was processed by melt mixing followed by compression molding (a two-step process resulting in fully molten and merged grains of the original HDPE powder, but higher exposure to thermooxidation), while the higher-viscosity UHMWPE could be processed only by compression molding (a single-step process leading to partially merged grains of the original UHMWPE powder, but lower oxidation [53]). Oxidative degradation of stabilized samples before e-beam irradiation was negligible (samples HDPE/α-Toc and UHWMPE/α-Toc; OI profiles in the 1st row of Fig. 15); this re-confirmed that phenolic stabilizers – including α-Toc – act as efficient antioxidants during thermooxidation that occurs during polymer processing. Oxidative degradation of both non-stabilized samples increased with time from e-beam irradiation (samples HDPE/0 and UHMWPE/0, lower rows of Fig. 15). The overall shape of the OI profiles was similar. The observed differences might have been attributed to the different molecular weights of the two polymers, their different crystallinities and/or processing-related effects (two-step vs. one-step preparation procedure for HDPE and UHMWPE samples, respectively). High oxidation of non-stabilized polyethylene samples after the application of ionizing radiation without the subsequent thermal treatment was described in numerous papers dealing with modification of UHMWPE for total joint replacements [32,51]. Oxidative degradation of stabilized samples was low, just very slightly increasing with time (samples HDPE/α-Toc and UHMWPE/α-Toc, lower rows of Fig. 15). In HDPE/α-Toc sample, the

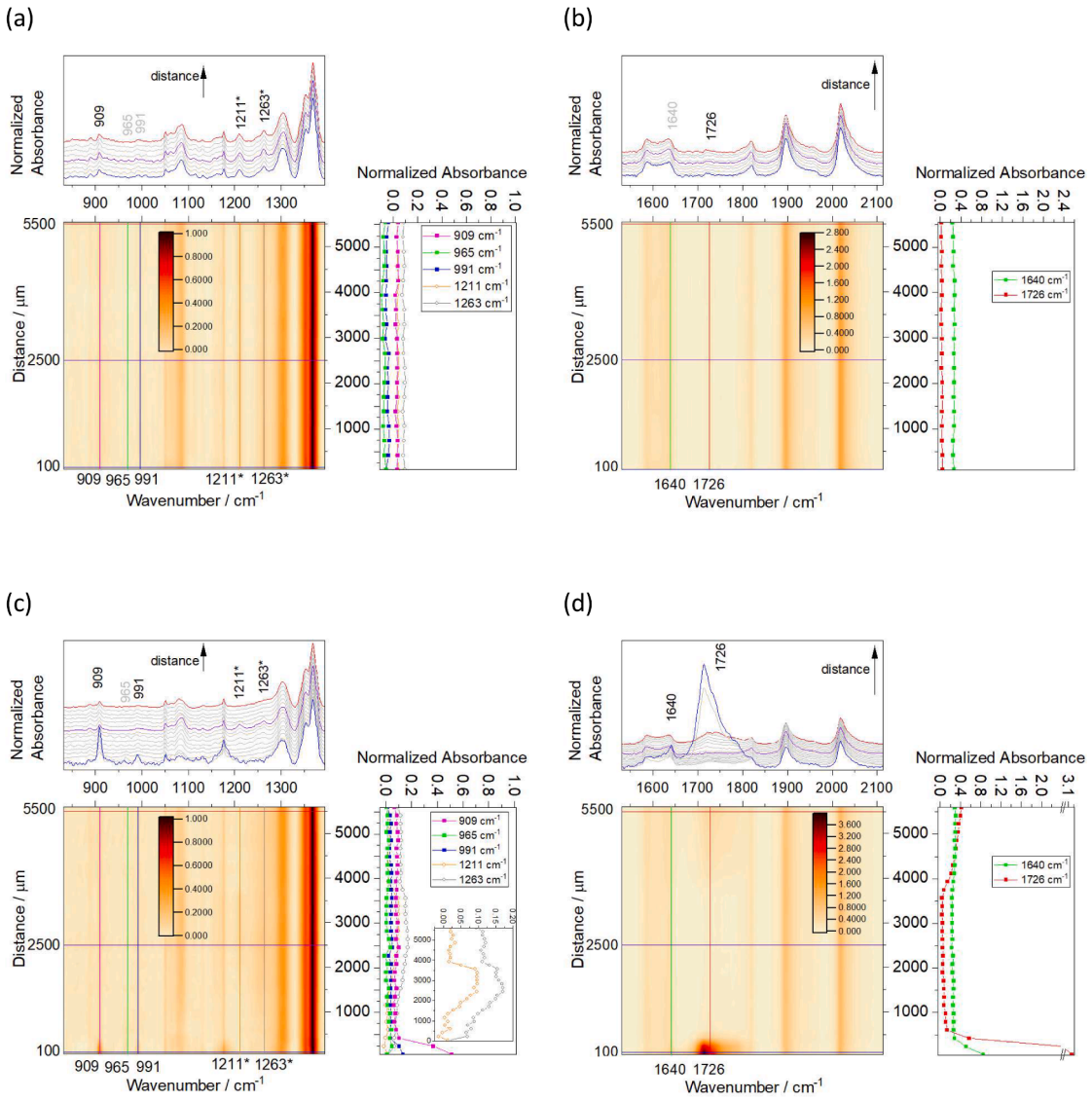

Fig. 11. 2D images of IR spectra as a function of distance from the exposed surface: (a, b) Spectra HDPE/α-Toc sample before WOM exposure. (c, d) Spectra of HDPE/α-Toc sample after 30 days of WOM exposure. Each of the four Figures (a–d) consists of a 2D-heatmap showing IR intensities, top plot showing a series of representative IR spectra, and left plot showing normalized absorbance of selected IR bands. All bands in the left Figures (a, c) and right Figures (b, d) were normalized to the same peak at 1380 cm^{-1} and 2020 cm^{-1}, respectively. The wavelengths of key peaks are marked in each image, α-Toc peaks are marked with the asterisk, and the grey font indicates that given peak is either weak or missing.

oxidation was a bit higher than in UHMWPE/α-Toc. We note that an analogous effect was observed for non-stabilized samples (oxidation in HDPE/0 was somewhat higher in comparison with UHMWPE/0). In conclusion, the results confirmed that α-Toc acted as an antioxidant for both types of polyethylene subjected to ionizing radiation.

The values of the trans-vinylene index are proportional to the absorbed radiation dose [54,55]. In non-irradiated samples (the first row of Fig. 15), the VI profiles were constant and close to zero, which confirmed that the original polyethylenes were regular aliphatic polyolefins, containing a minimal amount of C=C bonds. In the e-beam irradiated samples (the lower rows of Fig. 15), the VI values increased with the radiation dose in accordance with the literature [54,55]. The camel hump shape of VI profiles roughly corresponded to the intensity of e-beam interaction with the polymer matrix [56]. The overall shapes of VI profiles for HDPE and UHMWPE were slightly different, in analogy with OI profiles – this confirmed some small difference between the behavior of the two polyethylenes during the irradiation.

The crystallinity index profiles were almost constant and did not change after e-beam irradiation. HDPE exhibited higher average crystallinity than UHMWPE, which was in agreement with theoretical expectations – lower molecular weight polymer chains are easier to crystallize [57]. It is widely known that fast e-beam irradiation (typical irradiation times in minutes due to high e-beam dose rates) leads to the formation of crosslinks in the amorphous phase, whereas slower γ-irradiation or photooxidation in the air (typical irradiation times range from hours to weeks) results in scissions of the polyethylene chains [1,26,32,55]. Consequently, the crosslinks in the amorphous phase after e-beam irradiation acted as a steric hindrance, *preventing* further crystallization, while the chain scissions after UV irradiation released the entangled polymer chains and loops on the lamellar surfaces, *promoting* cold crystallization and leading to a small but observable crystallinity increase (compare CI in Figs. 9 and 15). As the crystallinity of HDPE and UHMWPE samples after e-beam irradiation did not change (Fig. 15, CI profiles) and crosslinking was shown to have a low impact on micromechanical properties [43,58], our parallel micromechanical measurements just confirmed that e-beam irradiation did not influence the mechanical performance (Fig. S2 in Supplementary materials). For the sake of completeness, we should note that the residual radicals in the

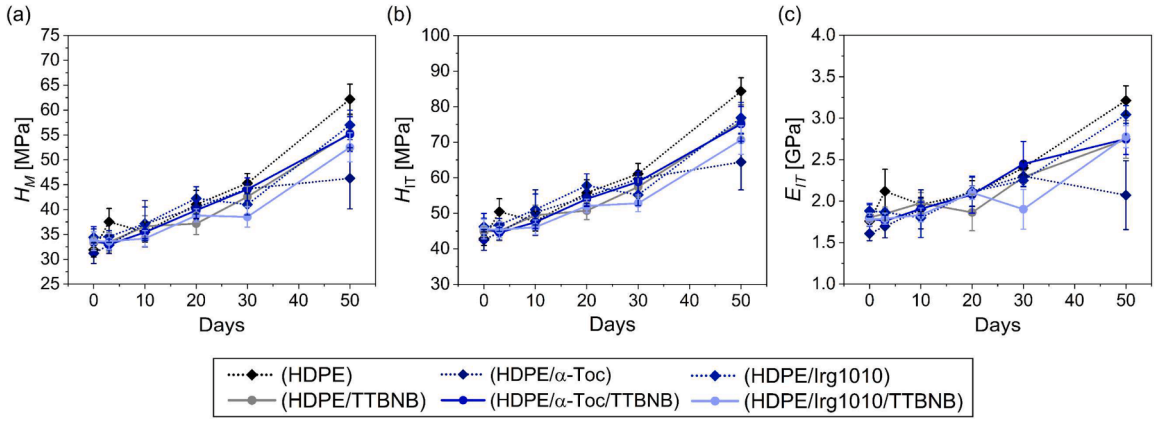

Fig. 12. Micromechanical properties of HDPE plaques with/without selected stabilizer (α-Toc or Irg1010) and/or spin-trapping agent (TTBNB): (a) Martens hardness, H_M, (b) indentation hardness, H_{IT}, and (c) indentation modulus, E_{IT}. All properties were measured at the WOM exposed surface. All quantities (H_{IT}, H_M and E_{IT}) are shown as a function of time (0, 3, 10, 20, 30 and 50 days of WOM exposure).

irradiated UHMWPE's without stabilization and remelting were shown to cause oxidative degradation in the long term [59], but the deterioration of mechanical performance was not observed within our time range.

3.4.2. *COC samples*

Fig. 16 documents that e-beam irradiation had a negligible impact on the COC structure. Almost the same IR/ATR spectra before and after e-beam irradiation were observed for both neat (Fig. 16a) and α-Toc stabilized sample (Fig. 16b). In accord with IR/ATR results, the micromechanical properties of COC samples after e-beam irradiation remained almost unchanged (Fig. S3 in Supplementary materials). Nevertheless, the COC samples after e-beam irradiation changed their color from white to yellow-brown; the change could be quantified by color analysis of light micrographs reproducibly (Fig. S4 in Supplementary materials).

4. Discussion

4.1. *Radicals formed in polyolefins subjected to non-ionizing radiation*

During photooxidation of PE compositions without TTBNB spin trap, practically no radicals have been detected either before or after irradiation. This indicated that the stability of polymer alkyl radicals, of adducts of the radicals with TTBNB and of α-tocopheroxyl radicals has been too low to be detected by classical CW ESR. The ESR spectra showed either no signal (pure HDPE) or minimal amounts of unidentified radicals (HDPE/α-Toc and HDPE/Irg1010) (Fig. 1). This finding was consistent with our previous study on HDPE samples stabilized with another natural phenolic stabilizer, (+)-catechin (CAT). In HDPE samples containing spin trap TTBNB (HDPE+TTBNB, HDPE+α-Toc+TTBNB, HDPE+Irg1010+TTBNB) paramagnetic spin adducts of polymer alkyl radicals with TTBNB has been detected before WOM exposure similarly as in the sample HDPE+CAT+TTBNB previously [3]. This observation has indirectly confirmed the generation of polymer alkyl radicals presumably by thermodegradation during the sample preparation procedure and partly trapping of these radicals by TTBNB.

WOM exposure has not increased the concentration of radicals in any of HDPE samples, on the contrary concentration of the mentioned adducts has decreased rapidly. It follows that the rest of the polymer alkyl radicals together with spin adducts created and radicals generated by incoming radiation during WOM exposure have participated in various reactions including oxidation (as proved by identification of oxidation products) and recombination processes and have disappeared fast regarding swift dynamics inside the polymer as a consequence of low T_g. In addition, the concentration of the spin adducts created has been limited by decreasing supplies of TTBNB.

ESR spectra of polymer alkyl radicals (doublets) generated in the initiation step of photooxidation have been observed in COC samples containing Irg1010 and TTBNB after WOM exposure (Fig. 4). Higher stability of polymer alkyl radicals in COC than in HDPE is caused by decreased dynamics inside COC due to its significantly higher T_g when compared with HDPE. In COC compositions subjected to photooxidation, both primary polymer alkyl radicals and α-tocopheroxyl radicals have been detected thanks to slower internal dynamics in COC than in PE compositions. The creation of the detectable radicals removed part of the reactive radicals from the chain photooxidation process but it could not stop it. At presence of α-Toc polymer alkyl radicals generated in COC samples have been quenched by α-Toc at simultaneous formation of stable α-tocopheroxyl radicals. α-tocopheroxyl radicals could be generated both by direct irradiation of α-Toc and by quenching of polymer radicals by α-Toc. Heterogeneous distribution of α-tocopheroxyl radicals in COC samples has been found by ESRI (Fig. 5). The distribution showed the highest concentration of radicals in the irradiated surface layer. Preferential scavenging of oxidized polymer alkyl radicals by α-Toc in oxygen rich surface layer of the polymer plates might explain this effect. A similar but lower effect has been observed in the back-surface layer probably due to the decreasing intensity of the radiation on its way through the polymer plate, which resulted in lower concentration of polymer alkyl radicals. Somewhat lower concentration of α-tocopheroxyl radicals observed in the samples stabilized with α-Toc + TTBNB has indicated that a part of polymer alkyl radicals generated during WOM exposure might be trapped by TTBNB and transformed to nonparamagnetic products subsequently. All radicals generated in COC by incoming radiation during WOM exposure have participated in various reactions including oxidation (as proved by identification of oxidation products) and recombination processes and have disappeared slowly regarding slow dynamics inside the polymer as a consequence of high T_g.

Weak ESR spectra of α-tocopheroxyl radical and spectra of immobilized nitroxide adducts of polymer radicals to TTBNB have been observed before WOM exposure (Fig. 3) in COC samples containing α-Toc (COC+α-Toc) and in COC samples containing TTBNB spin trap, respectively. Reactive radicals dissimilar to stable polymer alkyl radicals characterized by doublet ESR spectrum have been generated in COC by thermodegradation. In the presence of TTBNB the radicals have been partly captured by TTBNB creating observed spin adducts. In the presence of α-Toc α-tocopheroxyl radicals (α-Toc$^{\bullet}$) have been generated in the process of quenching the reactive radicals by α-Toc.

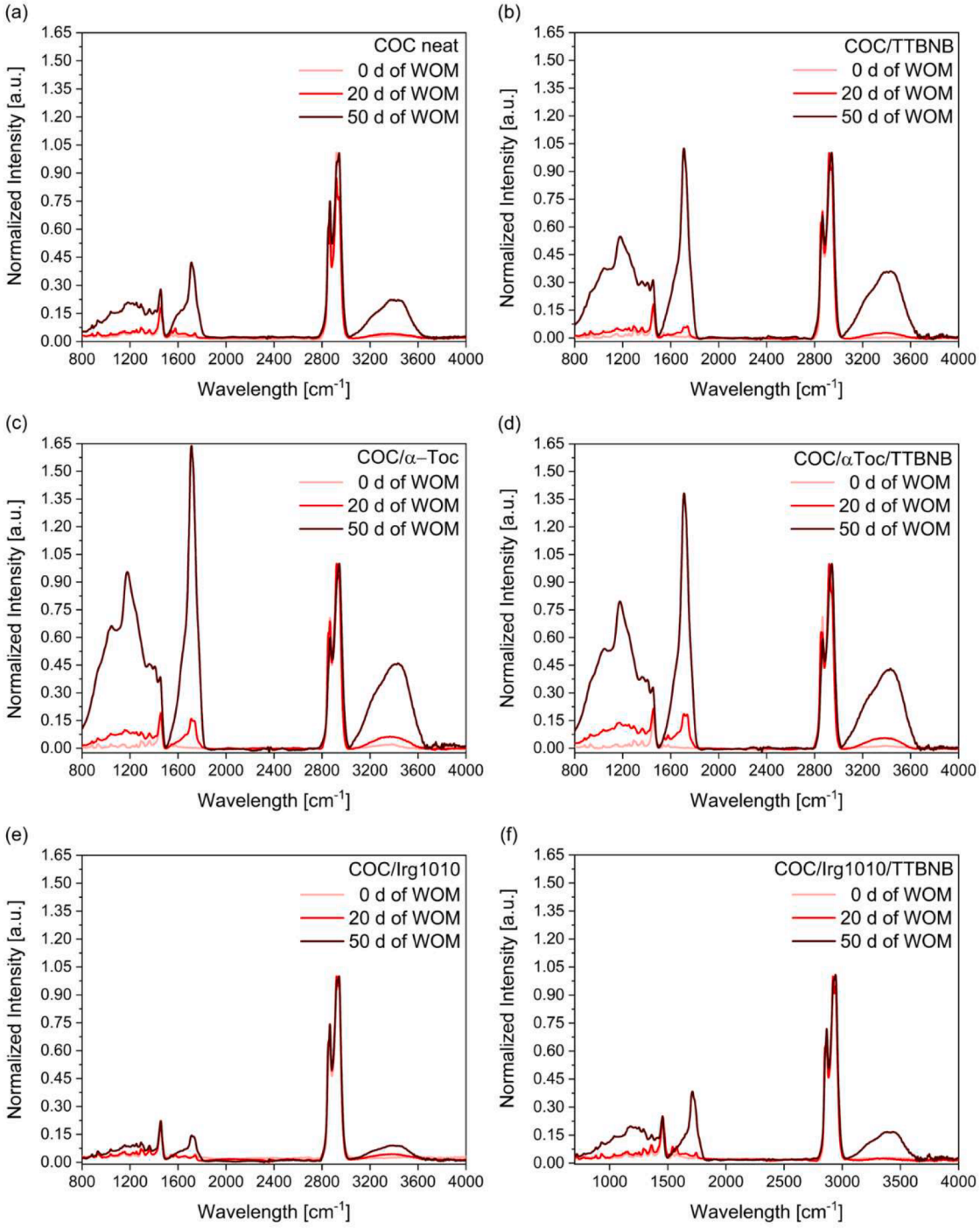

Fig. 13. IR/ATR spectra of COC samples before and after the WOM exposure: (a) neat COC, (b) COC/TTBNB, (c) COC/α-Toc, (d) COC/α-Toc/TTBNB, (e) COC/Irg1010, and (f) COC/Irg1010/TTBNB.

4.2. Radicals formed in polyolefins subjected to ionizing radiation

ESR proved that contrary to irradiation by non-ionizing radiation (WOM exposure) relatively stable polymer alkyl radicals have been generated in additive free HDPE and UHMWPE during irradiation by ionizing radiation (Fig. 6). Ionizing radiation generates polymer alkyl radicals $P^{\bullet}$ directly by removing electrons from polymer molecules. Such a process is able to generate polymer alkyl radicals anywhere inside the polymer block, even inside internal crystalline polymer locations, and not only in the vicinity of chromophoric centers as non-ionizing radiation can. The higher stability of polymer alkyl radicals generated by ionizing radiation when compared with non-ionizing radiation might be connected with the basic difference between mechanisms of radical generation exerted by ionizing and non-ionizing radiation. The concentration of the radicals has decreased with storage time. The radicals have been subjected to transformation reactions including oxidation processes resulting in the generation of various secondary radicals e.g. peroxyls and alkoxyls. Observed ESR spectra of such mixtures could not be analyzed.

In the UHMPWE and HDPE samples stabilized with 0.5 wt.% of α-Toc spectra of radical mixture similar to the spectra observed in the additive free samples after several days' storage have been observed shortly after

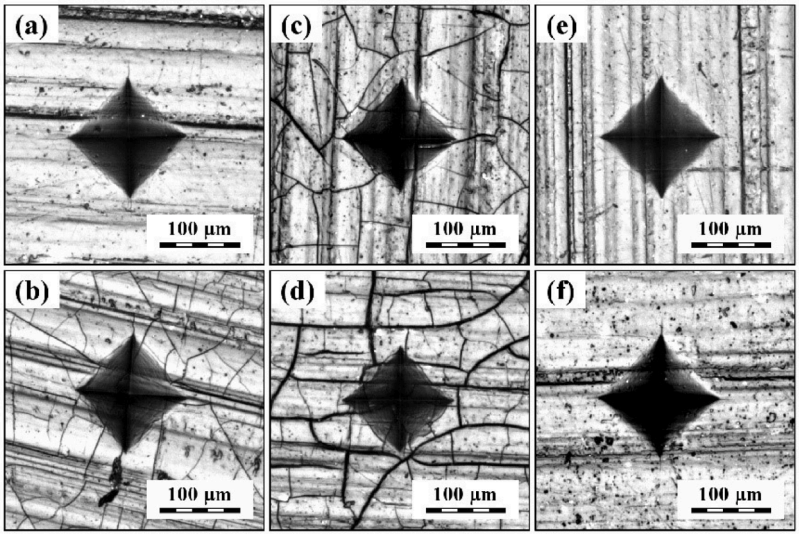

Fig. 14. Light micrographs showing surfaces of selected COC plaques after 50d of WOM exposure with imprints of indenter after MHI testing: (A) neat COC, (B) COC/TTBNB, (C) COC/αT-OH and (D) COC/αT-OH /TTBNB (E) COC/Irg1010 and (F) COC/Irg1010/TTBNB. The indentations were made with the instrumented MHI tester (maximum load 500 mN and dwell time = 60 s). The size of the indents was almost the same for all samples, confirming similar mechanical properties regardless of the different levels of the surface damage.

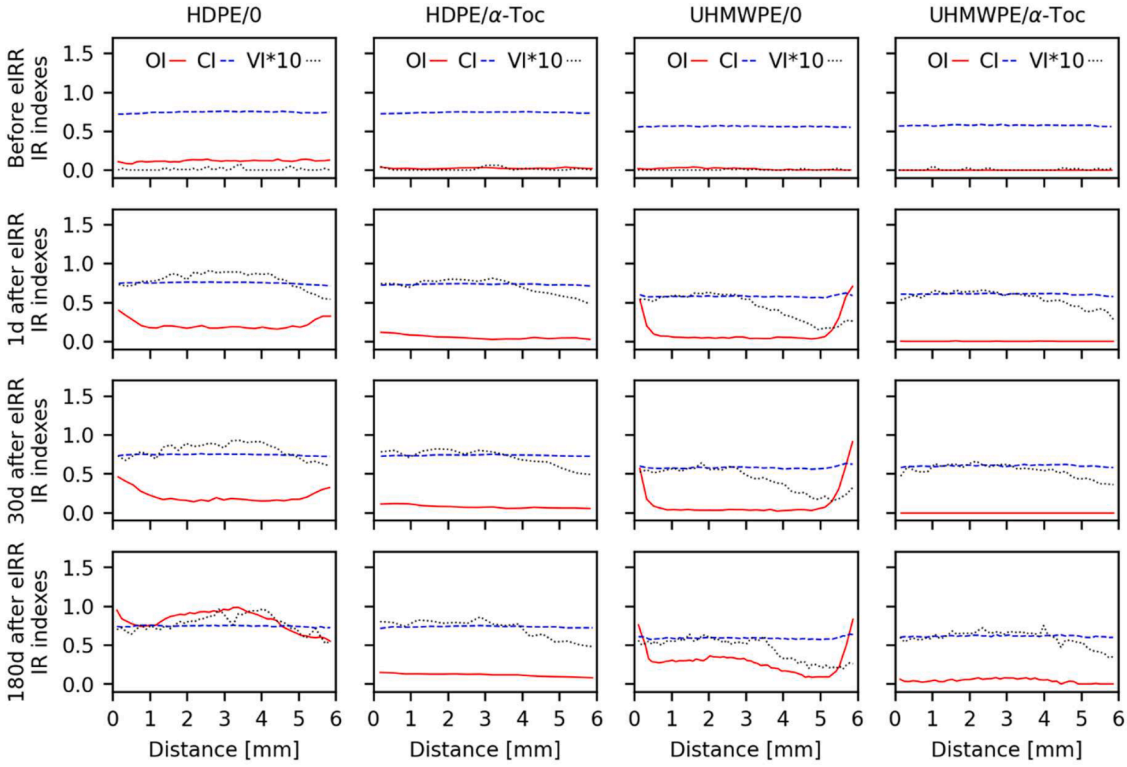

Fig. 15. Profiles of oxidation index (OI), crystallinity index (CI) and trans-vinylene index (VI) determined by IR microspectroscopy for polyethylene plaques (HDPE and UHMWPE) with or without stabilizer (α-Toc). The profiles are shown for various times of storage after e-beam irradiation exposure (0, 1, 30 and 180 days).

irradiation. Polymer radicals have probably been scavenged by α-Toc and created α-tocopheroxyl radicals have disappeared fast regarding swift dynamics inside the PE polymers as a consequence of low T_g. After exhausting α-Toc supplies radical transformation has continued in a similar way like in additive free polymers.

Broad line corresponding presumably to a mixture of polymer radicals, the concentration of which decreased with storage time, has been observed in the ESR spectrum of additive free COC sample irradiated by ionizing radiation. No distinct doublet type ESR spectra have been observed in the samples. ESR spectrum of stable α-tocopheroxyl radicals α-Toc$^{\bullet}$ has been observed in the COC sample stabilized with 0.5 wt.% of α-Toc after the same treatment. Concentration of α-tocopheroxyl radicals independent of storage time and representing roughly half of the concentration of α-tocopheroxyl radicals generated in the similar samples by non-ionizing radiation (WOM) has been found. Polymer radicals generated have probably been scavenged by α-Tocopherol similarly as in HDPE and UHMWPE polymers. Contrary to these polymers in COC α-tocopheroxyl radicals have been stable probably due to slow internal

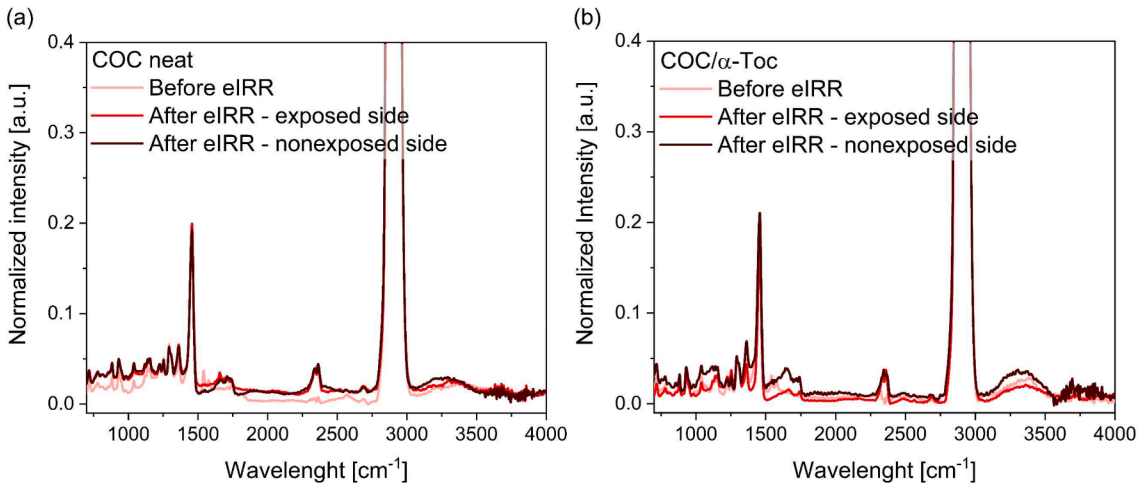

Fig. 16. IR/ATR spectra of COC samples before and after the e-beam irradiation: (a) neat COC, (b) COC/α-Toc. The spectra were measured 30 days after e-beam irradiation.

dynamics as a consequence of high T_g. Heterogeneous distribution of α-tocopheroxyl radicals in COC samples stabilized with α-Toc has been found by ESRI (Fig. 5c). The distribution has shown higher concentration of the radicals in both surface layers when compared with internal layers. Preferential scavenging of oxidized polymer alkyl radicals by α-Tocopherol in oxygen rich surface layers of the polymer plates may explain this effect. The clearly observed difference in behavior of COC samples exposed to non-ionizing radiation (high concentration of oxidation products) and ionizing e-beam irradiation (negligible oxidative degradation) may be connected with appearance of high concentration of well identified polymer alkyl radicals characterized by ESR doublet in the case of non-ionization irradiation (WOM exposure) in comparison with a mixture of unidentified radicals in the case of e-beam irradiation (compare Figs. 4 and 8).

4.3. Antioxidant and prooxidant activity phenolic stabilizers

The analysis of oxidation products enabled us to compare the activity of two phenolic stabilizers (α-Toc and Irg1010) in three polyolefins (HDPE, UHMWPE and COC) at three types of oxidative degradation: thermo-mechanical degradation (thermooxidation after melt mixing), degradation during long-term exposure to non-ionizing radiation (photooxidation during WOM aging), and degradation after short-term exposure to ionizing radiation (oxidation after e-beam irradiation). In several recent studies from both our group [1–3] and other researchers [4] and references therein, it has been shown that phenolic stabilizers can exhibit a surprising prooxidant activity during photooxidation and the expected antioxidant activity during thermooxidation. In this work, we confirmed and extended the abovementioned findings (Figs. 9–14) and compared the activity of α-Toc in polyolefins subjected to non-ionizing and ionizing radiation (Figs. 15, 16). The qualitative evaluation of all results (i.e. the combination of results from Figs. 9–16 related to samples containing α-Toc) is summarized in Table 3.

In addition, the results in this study enabled us to compare the activity of the natural phenolic stabilizers (α-Toc) and synthetic phenolic stabilizer (Irg1010) in the low-T_g polyolefin (HDPE) and high-T_g polyolefin (COC) subjected to non-ionizing radiation. These systems were studied with and without the presence of spin trapping agent (TTBNB) in order to catch unstable radicals that were formed during the process. Our results are summarized in Table 4.

The results in Tables 3 and 4 show that the behavior of phenolic stabilizes during various types of degradation of polyolefins is non-uniform. Both investigated phenolic stabilizers α-Toc and Irg1010 protected polyolefins HDPE and UHMWPE reliably against thermooxidation and ionizing radiation (Tables 3 and 4, Fig. 15). For COC, the situation was different. The COC polymer was resistant to thermooxidation and ionizing radiation even in its neat form (Fig. 16). As for non-ionizing radiation, the natural phenolic stabilizer α-Toc exhibited clear prooxidant activity in both HDPE and COC, whereas the synthetic phenolic stabilizer Irg1010 acted as a prooxidant in HDPE and antioxidant in COC (Figs. 9 and 13). Last but not least, even the spin trapping agent itself, TTBNB, exhibited ambiguous behavior: a slight antioxidant activity in HDPE systems (Fig. 9) and clear prooxidant activity in COC systems (Fig. 13). The ambiguous behavior of TTBNB documented that the somewhat exceptional pro-oxidant activity was not unique to phenolic stabilizers; it may occur during photooxidation of some other systems with non-phenolic stabilizers and/or radical scavengers as well, like in the above-described case of COC/TTBNB.

The complete explanation of the observed effects is unclear at the moment, although the fact that phenolic stabilizers can exhibit certain prooxidant activity in polymers subjected to non-ionizing radiation has been recently documented, as discussed above. Nevertheless, several facts are evident: (i) As for protection to non-ionizing radiation, synthetic HAS stabilizers (such as Tin770) are definitely better option than

Table 3
Behavior of α-Toc in various systems and at various types of degradation.

Degradation type	Behavior of α-Toc stabilizer		
	HDPE/α-Toc	UHMWPE/α-Toc	COC/α-Toc
Thermooxidation *	antioxidant	antioxidant	no effect
Non-ionizing radiation	prooxidant	prooxidant **	prooxidant
Ionizing radiation	antioxidant	antioxidant	no effect

* Thermooxidation data come from the comparison of oxidation indexes after melt mixing.

** Pro-oxidant activity of α-Toc in UHMWPE comes from parallel ongoing experiments; unpublished data.

Table 4
Behavior of phenolic stabilizers and spin trap in HDPE and COC systems subjected to non-ionizing radiation.

Polymer	Behavior of phenolic stabilizers and spin trapping agent during photooxidation				
	TTBNB	α-Toc	α-Toc/ TTBNB	Irg1010	Irg1010/ TTBNB
HDPE	weak antioxidant	prooxidant	prooxidant	prooxidant	prooxidant
COC	prooxidant	prooxidant	prooxidant	strong antioxidant	medium antioxidant

phenolic stabilizers, even though the usage of natural phenolic stabilizers (such as α-Toc or CAT) might be tempting for specific applications such as food packaging. (ii) As for protection to thermooxidation during polymer processing, the phenolic stabilizers are a safe and reliable choice. (iii) In general, the antioxidant and prooxidant activity of phenolic stabilizers depends on multiple factors, such as degradation type (thermooxidation, non-ionizing radiation and ionizing radiation; Table 3), polyolefin type (different radicals and mechanism in low-T_g and high-T_g polyolefins; Sections 4.1. and 4.2), stabilizer type (prooxidant and antioxidant activity of α-Toc and Irg1010 in COC, respectively; Table 4), polymer/stabilizer combination (prooxidant and antioxidant activity of Irg1010 in HDPE and COC, respectively; Table 4). (iv) Moreover, ESR results showed that the TTBNB spin trapping agent is able to quench polymer alkyl radicals by creating spin adducts with them, while α-Toc is able to quench polymer alkyl radicals by converting them to α-tocopheroxyl radicals. Additional remarks concerning the relations between the observed oxidation products and radicals during both ionizing and non-ionizing radiation are given in Supplementary materials.

4.4. Correlation between structure changes and micromechanical properties

The strongest changes of local mechanical properties were observed for HDPE samples exposed to non-ionizing radiation (Fig. 12). COC polymer was rather stiff (because it is an amorphous polymer studied well below its glass transition temperature, T_g) and its oxidation had negligible impact on its micromechanical behavior, even on the exposed surface (Figs. 14 and S1 in Supplementary materials). UHMWPE was subjected only to ionizing radiation, which did not affect the micromechanical performance of the polymer significantly (as briefly discussed above and documented in Figs. S2 and S3 in Supplementary materials).

According to both theoretical assumptions and previous experimental observations, the micromechanical properties of semicrystalline polymers measured high above their T_g (like in the case of HDPE) are affected mostly by their crystallinity, while other parameters (molecular weight, crosslinking, branching, entanglements etc.) play minor role [44,58]. Therefore, we decided to analyze the correlation between crystallinity and micromechanical performance of HDPE samples in more detail, in order to verify if our experimental data agree with

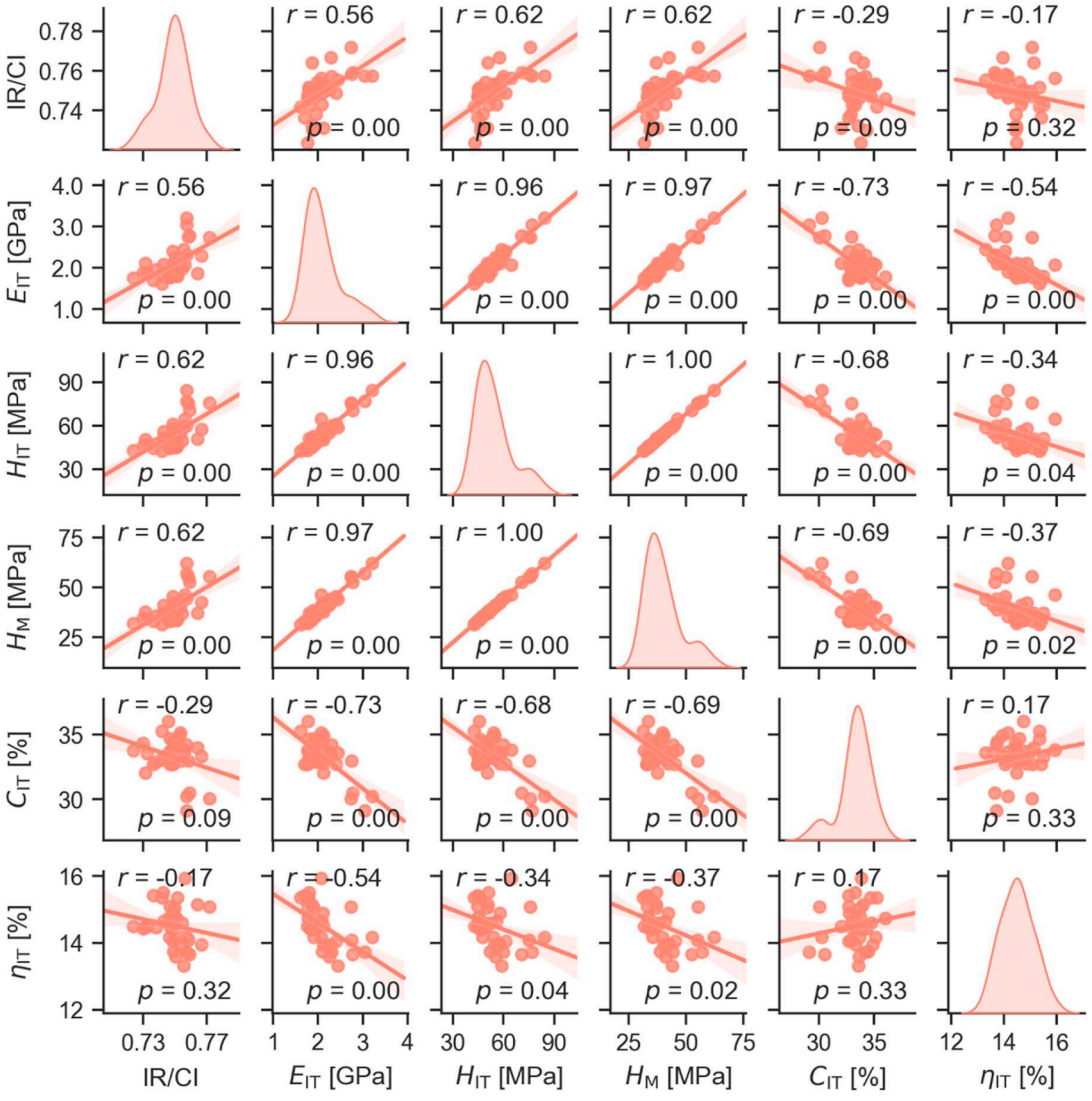

Fig. 17. Correlation between crystallinity (IR/CI; Section 2.6.1) and micromechanical properties (E_{IT}, H_{IT}, H_M, C_{IT}, and η_{IT}; Section 2.7) of HDPE samples. Diagonal elements of the scatterplot matrix graph show distribution of the measured quantities, whereas off-diagonal elements show correlations between each pair of quantities. The translucent bands around the regression lines represent 95 % confidence interval of the regression estimate. All off-diagonal plots show the values of Pearson's correlation coefficient *r* and *p*-values in the upper left corner and lower right corner, respectively.

theoretical predictions. The results of statistical analyses are summarized in the form of a scatterplot matrix graph (Fig. 17).

The scatterplot matrix graph (Fig. 17) shows correlations between all pairs of investigated quantities. Each correlation subplot contains two statistical descriptors: Pearson's correlation coefficient (r) and p-value (p) [47]. Briefly, the correlation coefficient ranges from +1 for perfect positive linear correlation (data points lie on a line with a positive slope), through zero (no linear dependency), to -1 for perfect negative linear correlation (data points lie on a line with a negative slope). The p-value represents the probability of obtaining the observed (or stronger) correlation just by coincidence; the results are regarded as statistically significant for $p < 0.05$ (i.e. below 5 %).

Micromechanical properties can be split into two groups [45]: stiffness-related (E_{IT}, H_{IT} and H_M) and viscosity-related (C_{IT} and η_{IT}). Fig. 17 documents that the strongest positive correlations ($r > 0.95$) were observed between all pairs of stiffness-related properties. This agreed with the pioneering theoretical studies of Tabor [60] and Struik [61], and their numerous experimental verifications [35]. Reasonably strong ($r > 0.55$) and statistically significant ($p < 0.01$) correlations were observed between all stiffness-related properties and the crystallinity. This was the key expected correlation as discussed above and elsewhere [45,62], which confirmed the reliability of our micromechanical characterization, i.e. the determination of crystallinity by means of IR microspectroscopy and the determination of micromechanical properties by means of microindentation hardness testing. The viscosity-related micromechanical properties did not change with crystallinity too much (both C_{IT} and η_{IT} varied by just a few percent) and their correlations with crystallinity and stiffness-related properties were either weak or even statistically insignificant ($p > 0.05$). Similar small changes were observed in previous studies [44,52] and could be attributed to the fact that viscosity-related properties are connected with polymer cold flow, which is unaffected by modest crystallinity changes.

5. Conclusions

We have studied the degradation processes of three bulk polyolefins (HDPE, UHMWPE and COC) subjected to non-ionizing radiation (terrestrial range of UV radiation) or ionizing radiation (high-energy electron beam). The polyolefins plaques were prepared by melt-mixing with or without phenolic stabilizers (natural α-tocopherol and synthetic Irganox®1010) and/or spin trapping agent (TTBNB; 2,4,6-Tri-*tert*-butylnitrosobenzene). This work is the first systematic comparison of the impact of the non-ionizing and ionizing radiation on polyolefins with phenolic stabilizers. We prepared as much as 18 different systems (Tables 1 and 2) and collected unusually high amount of experimental data about the radiation-generated radicals (Figs. 1–8; ESR and ESRI measurements) and the subsequent structure changes (Figs. 9–17; IR microspectroscopy and microindentation measurements). The main conclusions could be summarized as follows:

1. **The degradation processes in polyolefins subjected to non-ionizing and ionizing radiation are different.** Both non-ionizing and ionizing radiation generated polymer radicals in the whole volume of the irradiated samples, albeit by different mechanisms: low-energy non-ionizing radiation is supposed to activate hypothetical *chromophoric centers* in the polymer, which give rise to polymer alkyl radicals P*, while high-energy ionizing radiation can split polymer C-C bonds and generate the polymer radicals P* directly. The resulting alkyl radicals may be assumed to undergo analogous reactions, regardless of their origin. Nevertheless, this work has demonstrated that the stability of the generated radicals and the concentration of the subsequent radical-induced oxidation products depended not only on the mechanism of the radical generation, but also on the dynamics of polymer chains inside the studied polymers, which was closely related to their T_g.
2. **The phenolic stabilizers exhibit both antioxidant and prooxidant activity depending on the degradation type.** We have extended the conclusions from a few recent studies that revealed surprising prooxidant activity of some phenolic stabilizers in polyolefins subjected to non-ionizing radiation. Our results (summarized in Table 3) evidenced that natural phenolic stabilizer α-Toc exhibited *antioxidant* activity during thermooxidation (thermo-mechanical degradation during polymer processing), *prooxidant* activity during exposure to non-ionizing radiation (photooxidation; exposure to terrestrial range of UV radiation), and *antioxidant* activity during exposure to ionizing radiation (exposure to high-energy electrons). Moreover, the synthetic phenolic stabilizer Irg1010 showed similar, but not identical behavior during photooxidation (Table 4). All results confirmed that the degradation processes in polyolefins are complex and generalizations may lead to wrong conclusions. The activity of phenolic stabilizers depended not only on the degradation type (thermooxidation, non-ionizing or ionizing radiation), but also on type of polyolefin (low-T_g polyethylenes vs. high-T_g COC) and on the exact type of the stabilizer (α-Toc vs. Irg1010).
3. **The selected spin trapping agent, TTBNB, was stable enough to survive standard sample preparation by melt-mixing and catch short-living unstable radicals.** By means of TTBNB, we were able to catch short-living and unstable radicals in HDPE, which could not be detected in the previous studies. This finding may be useful for future work on similar systems containing low-T_g polymers (such as various types of very common polyethylene or polypropylene) containing highly dynamic polymer chains.

CRediT authorship contribution statement

Miroslav Šlouf: Conceptualization, Investigation, Methodology, Supervision, Writing – original draft, Writing – review & editing. **Veronika Gajdošová:** Data curation, Formal analysis, Investigation, Methodology, Visualization. **Ivana Šloufová:** Data curation, Formal analysis, Methodology, Validation. **Miroslava Lukešová:** Data curation, Investigation. **Danuše Michálková:** Investigation, Methodology, Validation. **Michael Thomas Müller:** Data curation, Formal analysis, Investigation, Methodology. **Jan Pilař:** Conceptualization, Data curation, Formal analysis, Investigation, Methodology, Supervision, Validation, Visualization, Writing – original draft, Writing – review & editing.

Declaration of competing interest

The authors declare that they have no known competing financial interests or personal relationships that could have appeared to influence the work reported in this paper.

Data availability

No data was used for the research described in the article.

Acknowledgment

Financial support through Grants NU21-06-00084 (Czech Health Research Council) and TREND FW01010564 (Technology Agency of Czech Republic) is gratefully acknowledged.

Supplementary materials

Supplementary material associated with this article can be found, in the online version, at doi:10.1016/j.polymdegradstab.2024.110708.

References

[1] J. Pilař, M. Šlouf, D. Michálková, I. Šloufová, T. Vacková, J. Dybal, Pro-oxidant activity of α-tocopherol during photooxidative degradation of polyolefins. ESRI and IR microspectroscopy studies, Polym. Degrad. Stab. 138 (2017) 55–71, https://doi.org/10.1016/j.polymdegradstab.2017.02.008.

[2] M. Šlouf, D. Michálková, V. Gajdošová, J. Dybal, J. Pilař, Prooxidant activity of phenolic stabilizers in polyolefins during accelerated photooxidation, Polym. Degrad. Stab. 166 (2019) 307–324, https://doi.org/10.1016/j.polymdegradstab.2019.06.013.

[3] V. Gajdošová, M. Šlouf, D. Michálková, J. Dybal, J. Pilař, Pro-oxidant activity of biocompatible catechin stabilizer during photooxidation of polyolefins, Polym. Degrad. Stab. 193 (2021) 109735, https://doi.org/10.1016/j.polymdegradstab.2021.109735.

[4] N.T. Dintcheva, G. Infurna, M. Baiamonte, F. D'Anna, Natural compounds as sustainable additives for biopolymers, Polymers 12 (2020) 732, https://doi.org/10.3390/polym12040732.

[5] K. Mukai, K. Nagai, A. Ouchi, T. Suzuki, K. Izumisawa, S. Nagaoka, Finding of remarkable synergistic effect on the aroxyl-radical-scavenging rates under the coexistence of α-tocopherol and catechins, Int. J. Chem. Kinet. 51 (2019) 643–656, https://doi.org/10.1002/kin.21284.

[6] M.D. Samper, E. Fages, O. Fenollar, T. Boronat, R. Balart, The potential of flavonoids as natural antioxidants and UV light stabilizers for polypropylene, J. Appl. Polym. Sci. 129 (2013) 1707–1716, https://doi.org/10.1002/app.38871.

[7] B. Qu, Y. Xu, W. Shi, B. Raanby, Photoinitiated crosslinking of low-density polyethylene. 6. Spin-trapping ESR studies on radical intermediates, Macromolecules 25 (1992) 5215–5219, https://doi.org/10.1021/ma00046a016.

[8] L. Chen, Q. Guo, S. Kutsuna, J. Mizukado, Determination of the mechanism of polymer thermolysis at low temperatures using spin trap electron spin resonance, Polymer 203 (2020) 122747, https://doi.org/10.1016/j.polymer.2020.122747.

[9] M. Sono, K. Kinashi, W. Sakai, N. Tsutsumi, Spin-trapping analysis and characterization of thermal degradation of thermoplastic poly(ether–ester) elastomer, Macromolecules 51 (2018) 1088–1099, https://doi.org/10.1021/acs.macromol.7b02654.

[10] S.M. Kurtz, UHMWPE Biomaterials Handbook: Ultra-High Molecular Weight Polyethylene in Total Joint Replacement and Medical Devices, 3rd ed., Elsevier/WA, William Andrew is an imprint of Elsevier, Amsterdam, Boston, 2016.

[11] M.S. Jahan, ESR insights into macroradicals in UHMWPE. UHMWPE Biomaterials Handbook, Elsevier, 2016, pp. 668–692, https://doi.org/10.1016/B978-0-323-35401-1.00035-1.

[12] S.I. Ohnishi, Y. Ikeda, M. Kashiwagi, I. Nitta, Electron spin resonance studies of irradiated polymers I. Factors affecting the electron spin resonance spectra of irradiated polymers, Polymer 2 (1961) 119–141, https://doi.org/10.1016/0032-3861(61)90017-9.

[13] S.I. Ohnishi, S.I. Sugimoto, I. Nitta, Electron spin resonance study of radiation oxidation of polymers. IIIA. Results for polyethylene and some general remarks, J. Polym. Sci. A Gen. Pap. 1 (1963) 605–623, https://doi.org/10.1002/pol.1963.100010204.

[14] N.S. Allen, Why do polymers degrade in sunlight, Trends Polym. Sci. 2 (1994) 366–375.

[15] N.C. Billingham, Localization of oxidation in polypropylene, Makromolekulare Chemie, Macromol. Symp. 28 (1989) 145–163, https://doi.org/10.1002/masy.19890280111.

[16] J. Pospíšil, Z. Horák, Z. Kruliš, S. Nešpůrek, The origin and role of structural inhomogeneities and impurities in material recycling of plastics, Macromol. Symp. 135 (1998) 247–263, https://doi.org/10.1002/masy.19981350127.

[17] J.F. Rabek, Polymer Photodegradation, Springer Netherlands, Dordrecht, 1995. http://link.springer.com/10.1007/978-94-011-1274-1. accessed October 23, 2023.

[18] H. Zweifel, Stabilization of Polymeric Materials, Springer Berlin Heidelberg, Berlin, Heidelberg, 1998. http://link.springer.com/10.1007/978-3-642-80305-5. accessed October 23, 2023.

[19] J. Pospíšil, P. Klemchuk, Photooxidation of polymers and its inhibition, in: Oxidation Inhibition in Organic Materials, 2, CRC PrESS, Boca Raton, Fla, 1990, pp. 29–162.

[20] G.A. George, M. Celina, Homogeneous and heterogeneous oxidation of polypropylene. Handbook of Polymer Degradation, 2nd ed., CRC Press, Boca Raton, 2000, pp. 277–314.

[21] N.C. Billingham, The physical chemistry of polymer oxidation and stabilization. Atmospheric Oxidation and Antioxidants, 2nd ed., Elsevier, Amsterdam, 1993, pp. 219–277.

[22] J.L. Gardette, Fundamentals and technical aspects of the photooxidation of polymers. Handbook of Polymer Degradation, 2nd ed., CRC Press, Boca Raton, 2000, pp. 671–698.

[23] A. Marek, L. Kaprálková, P. Schmidt, J. Pfleger, J. Humlíček, J. Pospíšil, J. Pilař, Spatial resolution of degradation in stabilized polystyrene and polypropylene plaques exposed to accelerated photodegradation or heat aging, Polym. Degrad. Stab. 91 (2006) 444–458, https://doi.org/10.1016/j.polymdegradstab.2005.01.048.

[24] J. Pilař, D. Michálková, I. Šeděnková, J. Pfleger, J. Pospíšil, NOR and nitroxide-based HAS in accelerated photooxidation of carbon-chain polymers; Comparison with secondary HAS: an ESRI and ATR FTIR study, Polym. Degrad. Stab. 96 (2011) 847–862, https://doi.org/10.1016/j.polymdegradstab.2011.02.004.

[25] J. Pilař, D. Michálková, M. Šlouf, T. Vacková, J. Dybal, Heterogeneity of accelerated photooxidation in commodity polymers stabilized by HAS: ESRI, IR, and MH study, Polym. Degrad. Stab. 103 (2014) 11–25, https://doi.org/10.1016/j.polymdegradstab.2014.02.019.

[26] J. Pilař, D. Michálková, M. Šlouf, T. Vacková, Long-term accelerated weathering of HAS stabilized PE and PP plaques: compliance of ESRI, IR, and microhardness data characterizing heterogeneity of photooxidation, Polym. Degrad. Stab. 120 (2015) 114–121, https://doi.org/10.1016/j.polymdegradstab.2015.06.011.

[27] P. Bracco, E. Oral, Vitamin E-stabilized UHMWPE for total joint implants: a review, Clin. Orthop. Relat. Res. 469 (2011) 2286–2293, https://doi.org/10.1007/s11999-010-1717-6.

[28] E. Oral, O.K. Muratoglu, Highly cross-linked UHMWPE doped with vitamin E. UHMWPE Biomaterials Handbook, Elsevier, 2016, pp. 307–325. https://linkinghub.elsevier.com/retrieve/pii/B9780323354011000181. accessed October 23, 2023.

[29] H. Dorschner, U. Lappan, K. Lunkwitz, Electron beam facility in polymer research: radiation induced functionalization of polytetrafluoroethylene, Nucl. Instrum. Methods Phys. Res. Sect. B Beam Interact. Mater. At. 139 (1998) 495–501, https://doi.org/10.1016/S0168-583X(97)00937-3.

[30] H. Dorschner, W. Jenschke, K. Lunkwitz, Radiation field distributions of an industrial electron beam accelerator, Nucl. Instrum. Methods Phys. Res. Sect. B Beam Interact. Mater. At. 161–163 (2000) 1154–1158, https://doi.org/10.1016/S0168-583X(99)00811-3.

[31] V. Premnath, A. Bellare, E.W. Merrill, M. Jasty, W.H. Harris, Molecular rearrangements in ultra high molecular weight polyethylene after irradiation and long-term storage in air, Polymer 40 (1999) 2215–2229, https://doi.org/10.1016/S0032-3861(98)00438-8.

[32] M. Slouf, H. Synkova, J. Baldrian, A. Marek, J. Kovarova, P. Schmidt, H. Dorschner, M. Stephan, U. Gohs, Structural changes of UHMWPE after e-beam irradiation and thermal treatment, J. Biomed. Mater. Res. 85B (2008) 240–251, https://doi.org/10.1002/jbm.b.30942.

[33] A. Marek, EPR study of diffusion processes in polymer systems, Ph.D. Thesis, Charles University, Prague, 2006. https://dspace.cuni.cz/handle/20.500.11956/95058 (accessed February 6, 2023).

[34] L. Costa, I. Carpentieri, P. Bracco, Post electron-beam irradiation oxidation of orthopaedic Ultra-High Molecular Weight Polyethylene (UHMWPE) stabilized with vitamin E, Polym. Degrad. Stab. 94 (2009) 1542–1547, https://doi.org/10.1016/j.polymdegradstab.2009.04.023.

[35] M. Slouf, S. Arevalo, H. Vlkova, V. Gajdosova, V. Kralik, L. Pruitt, Comparison of macro-, micro- and nanomechanical properties of clinically-relevant UHMWPE formulations, J. Mech. Behav. Biomed. Mater. 120 (2021) 104205, https://doi.org/10.1016/j.jmbbm.2020.104205.

[36] F.J. Medel, C.M. Rimnac, S.M. Kurtz, On the assessment of oxidative and microstructural changes after *in vivo* degradation of historical UHMWPE knee components by means of vibrational spectroscopies and nanoindentation, J. Biomed. Mater. Res. 89A (2009) 530–538, https://doi.org/10.1002/jbm.a.31992.

[37] M. Slouf, T. Vackova, M. Nevoralova, D. Pokorny, Micromechanical properties of one-step and sequentially crosslinked UHMWPEs for total joint replacements, Polym. Test. 41 (2015) 191–197, https://doi.org/10.1016/j.polymertesting.2014.12.003.

[38] S. Kim, P.H. Kang, Y.C. Nho, O.B. Yang, Effect of electron beam irradiation on physical properties of ultrahigh molecular weight polyethylene, J. Appl. Polym. Sci. 97 (2005) 103–116, https://doi.org/10.1002/app.21734.

[39] M. Slouf, V. Gajdosova, J. Dybal, R. Sticha, P. Fulin, D. Pokorny, J. Mateo, J. J. Panisello, V. Canales, F. Medel, A. Bistolfi, P. Bracco, European database of explanted UHMWPE liners from total joint replacements: correlations among polymer modifications, structure, oxidation, mechanical properties and lifetime *in vivo*, Polymers 15 (2023) 568, https://doi.org/10.3390/polym15030568.

[40] W.C. Oliver, G.M. Pharr, An improved technique for determining hardness and elastic modulus using load and displacement sensing indentation experiments, J. Mater. Res. 7 (1992) 1564–1583, https://doi.org/10.1557/JMR.1992.1564.

[41] W.C. Oliver, G.M. Pharr, Nanoindentation in materials research: past, present, and future, MRS Bull. 35 (2010) 897–907, https://doi.org/10.1557/mrs2010.717.

[42] A.C. Fischer-Cripps, Nanoindentation, Springer New York, New York, NY, 2004. http://link.springer.com/10.1007/978-1-4757-5943-3. accessed October 23, 2023.

[43] M. Slouf, B. Strachota, A. Strachota, V. Gajdosova, V. Bertschova, J. Nohava, Macro-, micro- and nanomechanical characterization of crosslinked polymers with very broad range of mechanical properties, Polymers 12 (2020) 2951, https://doi.org/10.3390/polym12122951.

[44] M. Slouf, J. Krajenta, V. Gajdosova, A. Pawlak, Macromechanical and micromechanical properties of polymers with reduced density of entanglements, Polym. Eng. Sci. 61 (2021) 1773–1790, https://doi.org/10.1002/pen.25699.

[45] M. Slouf, S. Henning, Micromechanical properties, in: H.F. Mark (Ed.), Encyclopedia of Polymer Science and Technology, 3rd ed., Wiley, 2022: pp. 1–50. https://onlinelibrary.wiley.com/doi/10.1002/0471440264.pst199.pub2 (accessed October 23, 2023).

[46] J. VanderPlas, Python Data Science Handbook: Essential Tools for Working With Data, 1st ed., O'Reilly, 2016. Beijing Boston Farnham Sebastopol Tokyo.

[47] T.C. Urdan, Statistics in Plain English, 4th ed., Routledge, Taylor & Francis Group, New York, NY, 2017.

[48] M. Gardette, A. Perthue, J.L. Gardette, T. Janecska, E. Földes, B. Pukánszky, S. Therias, Photo- and thermal-oxidation of polyethylene: comparison of mechanisms and influence of unsaturation content, Polym. Degrad. Stab. 98 (2013) 2383–2390, https://doi.org/10.1016/j.polymdegradstab.2013.07.017.

[49] S. Spiegelberg, A. Kozak, G. Braithwaite, Characterization of physical, chemical, and mechanical properties of UHMWPE. UHMWPE Biomaterials Handbook,

Elsevier, 2016, pp. 531–552. https://linkinghub.elsevier.com/retrieve/pii/B9780323354011000296. accessed October 23, 2023.
[50] L. Costa, P. Bracco, Mechanisms of cross-linking, oxidative degradation, and stabilization of UHMWPE. UHMWPE Biomaterials Handbook, Elsevier, 2016, pp. 467–487. https://linkinghub.elsevier.com/retrieve/pii/B9780323354011000260. accessed October 23, 2023.
[51] F. Lednický, M. Šlouf, J. Kratochvíl, J. Baldrian, D. Novotná, Crystalline character and microhardness of gamma-irradiated and thermally treated UHMWPE, J. Macromol. Sci. Part B 46 (2007) 521–531, https://doi.org/10.1080/00222340701257778.
[52] M. Slouf, E. Pavlova, S. Krejcikova, A. Ostafinska, A. Zhigunov, V. Krzyzanek, P. Sowinski, E. Piorkowska, Relations between morphology and micromechanical properties of alpha, beta and gamma phases of iPP, Polym. Test. 67 (2018) 522–532, https://doi.org/10.1016/j.polymertesting.2018.03.039.
[53] C. Bucknall, V. Altstädt, D. Auhl, P. Buckley, D. Dijkstra, A. Galeski, C. Gögelein, U. A. Handge, J. He, C.Y. Liu, G. Michler, E. Piorkowska, M. Slouf, I. Vittorias, J. J. Wu, Structure, processing and performance of ultra-high molecular weight polyethylene (IUPAC Technical Report). Part 2: crystallinity and supra molecular structure, Pure Appl. Chem. 92 (2020) 1485–1501, https://doi.org/10.1515/pac-2019-0403.
[54] M. Fung, J.G. Bowsher, D.W. Van Citters, Variation of mechanical properties and oxidation with radiation dose and source in highly crosslinked remelted UHMWPE, J. Mech. Behav. Biomed. Mater. 82 (2018) 112–119, https://doi.org/10.1016/j.jmbbm.2018.03.005.
[55] M. Slouf, J. Mikesova, J. Fencl, H. Stara, J. Baldrian, Z. Horak, Impact of dose-rate on rheology, structure and wear of irradiated UHMWPE, J. Macromol. Sci. Part B 48 (2009) 587–603, https://doi.org/10.1080/00222340902837824.
[56] M.T. Müller, C. Zschech, M. Gedan-Smolka, M. Pech, R. Streicher, U. Gohs, Surface modification and edge layer post curing of 3D sheet moulding compounds (SMC), Radiat. Phys. Chem. 173 (2020) 108872, https://doi.org/10.1016/j.radphyschem.2020.108872.
[57] L.J. Tung, S. Buckser, The effects of molecular weight on the crystallinity of polyethylene, J. Phys. Chem. 62 (1958) 1530–1534, https://doi.org/10.1021/j150570a015.
[58] F.J. Balta-Calleja, S. Fakirov, Microhardness of Polymers, Cambridge University Press, Cambridge, England, 2000.
[59] P. Bracco, A. Bellare, A. Bistolfi, S. Affatato, Ultra-high molecular weight polyethylene: influence of the chemical, physical and mechanical properties on the wear behavior. A review, Materials 10 (2017) 791, https://doi.org/10.3390/ma10070791.
[60] D. Tabor, The Hardness of Metals, Clarendon Press; Oxford University Press, Oxford, New York, 1951.
[61] L.C.E. Struik, Some problems in the non-linear viscoelasticity of amorphous glassy polymers, J. Non Cryst. Solids 131–133 (1991) 395–407, https://doi.org/10.1016/0022-3093(91)90333-2.
[62] A. Flores, F. Ania, F.J. Baltá-Calleja, From the glassy state to ordered polymer structures: a microhardness study, Polymer 50 (2009) 729–746, https://doi.org/10.1016/j.polymer.2008.11.037.